

On the relative performance of some parametric and nonparametric estimators of option prices

Carlo Marinelli* and Stefano D'Addona†

November 28, 2024

Abstract

We examine the empirical performance of some parametric and nonparametric estimators of prices of options with a fixed time to maturity, focusing on variance-gamma and Heston models on one side, and on expansions in Hermite functions on the other side. The latter class of estimators can be seen as perturbations of the classical Black-Scholes model. The comparison between parametric and Hermite-based models having the same “degrees of freedom” is emphasized. The main criterion is the out-of-sample relative pricing error on a dataset of historical option prices on the S&P500 index. Prior to the main empirical study, the approximation of variance-gamma and Heston densities by series of Hermite functions is studied, providing explicit expressions for the coefficients of the expansion in the former case, and integral expressions involving the explicit characteristic function in the latter case. Moreover, these approximations are investigated numerically on a few test cases, indicating that expansions in Hermite functions with few terms achieve competitive accuracy in the estimation of Heston densities and the pricing of (European) options, but they perform less effectively with variance-gamma densities. On the other hand, the main large-scale empirical study show that parsimonious Hermite estimators can even outperform the Heston model in terms of pricing errors. These results underscore the trade-offs inherent in model selection and calibration, and their empirical fit in practical applications.

1 Introduction

Our main goal is to test the empirical performance in the estimation of option prices of some well-known parametric model for the density of logarithmic asset prices versus nonparametric approximations of the same density by means of expansions in (shifted and rescaled) Hermite functions. We are particularly interested in comparisons among parametric and nonparametric models having, in a certain sense, the same degrees of freedom. In fact, if the density to be approximated is square-integrable, i.e. it belongs to $L^2 := L^2(\mathbb{R})$, then it admits an expansion in Hermite functions, a truncation of which depends only on a finite number of real coefficients. This approximation is nonparametric in the sense that it does not assume that the density belongs to any parametric class. As benchmark parametric models for the density of logarithmic returns we consider the variance-gamma model, as defined in [9], and the Heston model (see [7]), the former of which is specified by three parameters and the latter by five (see §§4-5 for details). Denoting the density of logarithmic returns at a fixed time t by f , and assuming that f belongs to L^2 , we shall consider approximations of f of the type

$$f_n(x) := \sum_{k=0}^n \alpha_k h_k \left(\frac{x-b}{a} \right),$$

*Department of Mathematics, University College London, Gower Street, London WC1E 6BT, UK.

†Dipartimento di Scienze Politiche, Università degli studi Roma Tre, via G. Chiabrera 199, 00145 Roma, Italy.

where h_k is the Hermite functions of order k defined by $h_k(x) = H_k(\sqrt{2}x) \exp(-x^2/2)$, with H_k the Hermite polynomial of degree k , the coefficients (α_k) are real numbers, and the constants a, b are scale and location parameters, respectively (see §3 for details). For every integer n , a function f_n is determined by $n+3$ parameters, to wit, the $n+1$ coefficients (α_k) and the scale and location parameters a and b . This class of approximations and some of its properties were studied in [12], where it was observed that f_n can be seen as a perturbation of a Gaussian density (corresponding to $n = 0$), or, in other words, of the classical Black-Scholes model. Assuming that the reference probability measure is a pricing measure, it was also observed that setting $b = -a^2/2$, as is necessary in the limiting case $n = 0$, does not significantly alter the empirical accuracy of the approximation. Therefore we shall mostly restrict to this specific setting, in which case the approximation $f_{n,p}$, defined as f_n with $b = -a^2/2$, is uniquely determined by $n+2$ parameters. In general neither f_n nor $f_{n,p}$ are themselves densities, as they may assume negative values on nonempty subsets of \mathbb{R} and do not necessarily integrate to one. Similarly, assuming for simplicity (and without loss of generality) that the asset price is equal to one at time zero, the function $x \mapsto e^x f(x)$ integrates to one, but the same cannot be expected to hold replacing f by f_n or $f_{n,p}$. It turns out that the two constraints on approximations of f to integrate to one and to integrate to one when multiplied by the exponential function are independent and reduce the degrees of freedom by two. A Hermite approximation of f satisfying these two constraints will be said to have the approximate martingale property. An approximation of the type $f_{n,p}$ with the approximate martingale property, that will be denoted by $f_{n,m}$, is then uniquely determined by n parameters. Natural matches for parametric models of the density depending on n parameters are then f_{n-3} , $f_{n-2,p}$, and $f_{n,m}$, whenever these are well defined. In particular, we shall test, on the basis of several criteria, the variance-gamma model against $f_{1,p}$ and $f_{3,m}$, and the Heston model against f_2 , $f_{3,p}$ and $f_{5,m}$. This can also be seen as an attempt to understand whether a general-purpose approximation scheme can reproduce, with reasonable accuracy, “informed” parametric models especially designed for financial asset returns.

The empirical evidence that we obtain from numerical experiments on simulated and real data is somewhat mixed. The density of a variance-gamma process, that, incidentally, does not belong to L^2 at small times, appears to be harder to approximate with a good level of precision than the density of a Heston process, both in terms of the L^2 norm of the difference between the target density and the approximating one and in terms of the pricing error. More precisely, option prices implied by a Heston density can be approximated quite well by Hermite estimators, while the results are poorer for option prices implied by a variance-gamma density, even though some estimators perform well in particular cases. In an extensive empirical study on real data, where all estimators are compared on the basis of their out-of-sample pricing error, it turns out, as expected, that the richer (in terms of number of parameters) Heston model performs better than the variance-gamma model, but, rather surprisingly, a simple approximation of the implicit density of logarithmic returns of type f_2 , hence a linear combination of very few scaled and shifted Hermite functions, outperforms also the Heston model.

Another motivation for the empirical study conducted here is to complement the results of our previous work [12], where several Hermite-based nonparametric option price estimators were compared to each other as well as to an elementary nonparametric method relying on linear interpolation on the implied volatility curve, but no comparison with nontrivial well-established parametric models was carried out. Even though [12] considered more Hermite-based approximations than those used here, results are directly and easily comparable with those reported therein.

While we only deal with approximations of densities of logarithmic returns at fixed times, it would of course be interesting to study the (presumably much harder) problem of approximating joint densities at multiple times by nonparametric models based on Hermite functions. The closely related problem of estimating prices of options with different maturities by a unique time-dependent Hermite-based model is of course equally interesting, especially in view of the well-known fact that the Heston model performs reasonably well in the approximation of prices

of options with medium-long maturity.

Some literature on financial applications of Hermite functions, as well as of other basis functions involving orthogonal polynomials, is cited in [12], to which we refer. Other examples are [1] and the very recent [15], that also contains references to applications of the related Gram–Charlier type A series. The type of problems treated in all these references, however, is different from ours. Applications of Hermite polynomials to some classical statistical problems and relevant pointers to the literature can be found, e.g., in [14].

We conclude this introductory section with a brief outline of the rest of the text: after fixing some basic notation and assumptions in §2, we recall the definition of the Hermite option price estimator in §3, referring to [12] for more details. Sections 4 and 5 contain brief presentations of the variance-gamma and Heston processes, including sufficient conditions for their densities to belong to L^2 , and of the corresponding option pricing formulas used throughout. Some theoretical aspects of the expansions in series of Hermite functions of logarithmic returns’ densities are studied in §6. In particular, the smoothness of the objective function arising in the optimization of f_n with respect to the parameters a, b is proved and its first- and second-order total derivatives are computed. Moreover, the coefficients of a constrained Hermite expansion in terms of those of an unconstrained expansion are characterized explicitly. Furthermore, it is shown that, in the variance-gamma case, the coefficients of the Hermite expansion of a density can be computed in terms of integrals with respect to gamma measures, while, in the Heston case, they can be obtained by the Hermite expansion of an explicit function involving the Fourier transform of the density, which is known in closed form. In the final section 7, results of numerical computations on synthetic and real data are reported and discussed. We first consider two test cases, where a variance-gamma density and a Heston density, as well as a set of corresponding option prices, are estimated by the Hermite approximation schemes described above. Then we provide a comparison of the empirical performance of all the parametric models and Hermite approximations on S&P500 option data, by analyzing the respective out-of-sample pricing errors.

2 Preliminaries

2.1 Notation and basic assumptions

We shall use the following notation: $\mathbb{R}_+ := [0, +\infty[$, $\mathbb{R}_+^\times := \mathbb{R}_+ \setminus \{0\}$, and $A \lesssim B$ to mean that there exists a constant c such that $A \leq cB$, with subscripts indicating parameters on which c depends. Moreover, $A \approx B$ stands for $A \lesssim B$ and $B \lesssim A$. Numbers will be reported with three significant digits, with the exception of Tables 11 and 12 (for formatting reasons). The spaces $L^p(\mathbb{R})$, $p \in [0, \infty]$, are denoted simply by L^p . The scalar product of two functions $f, g \in L^2$ is denoted by $\langle f, g \rangle$. The distribution function and the density function of the standard Gaussian measure on \mathbb{R} are denoted by Φ and ϕ , respectively. The few special functions used in the text are defined as in [13].

Let $T \in \mathbb{R}_+^\times$ and $(\Omega, \mathcal{F}, \mathbb{P})$ be a probability space endowed with a right-continuous filtration $(\mathcal{F}_t)_{t \in [0, T]}$ such that \mathcal{F}_0 contains the negligible sets of \mathcal{F}_T . All random variables and stochastic processes will be defined on this filtered probability space. The expectation (with respect to \mathbb{P}) of a random variable X will be denoted by $\mathbb{P}X$.

Regarding asset price processes, independently of the setting considered in the following sections, we shall use the following conventions: \tilde{S} stands for the price process of a dividend-paying asset, and β for the price process of a money market account used as numéraire, about which we assume that

$$\beta_t =: \exp\left(\int_0^t r_u du\right),$$

where r , the short rate process, is positive and adapted. The discounted asset price process is then defined by $S := \tilde{S}/\beta$. The cumulative dividend process is assumed, for simplicity, to be determined by a constant non-random dividend rate q , and that the process $(S_t e^{qt})_{t \geq 0}$ is a

martingale with a respect to a probability measure \mathbb{Q} , equivalent to \mathbb{P} , that is used as pricing measure.

The function $\text{BS}: \mathbb{R}_+^6 \rightarrow \mathbb{R}_+$ is defined, for every $(s_0, k, r, q, \sigma, t)$, as the Black-Scholes price at time zero of a put option with strike k and expiration time t on an asset with price s at time zero, volatility σ , and dividend rate q , assuming a constant short rate equal to r .

For later reference, we recall a convergence result proved in [11]: for a function $f \in L^1 \cap L^2$, let $\pi: \mathbb{R}_+ \rightarrow \mathbb{R}_+$ be defined by

$$\pi(k) := \int_{\mathbb{R}} (k - e^x)^+ f(x) dx.$$

If (f_n) is a sequence of functions in $L^1 \cap L^2$ converging to f in L^2 , then, defining π_n in the obvious way, one has, for any $k_0 \in \mathbb{R}_+^\times$,

$$\pi(k) = \frac{k}{k_0} \pi(k_0) + \lim_{n \rightarrow \infty} \left(\pi^n(k) - \frac{k}{k_0} \pi^n(k_0) \right).$$

For a given $n \in \mathbb{N}$, in the approximation

$$\begin{aligned} \pi(k) &\approx \frac{k}{k_0} \pi(k_0) + \pi^n(k) - \frac{k}{k_0} \pi^n(k_0) \\ &= \pi^n(k) + \frac{k}{k_0} (\pi(k_0) - \pi^n(k_0)) \end{aligned} \tag{2.1}$$

we shall say that the right-hand side is a ‘‘corrected’’ version of $\pi(k)$ once $\pi(k_0)$ is known.

3 Hermite estimator

The Hermite estimator of option prices is constructed approximating the density of logarithmic returns by a finite linear combination of Hermite functions. The procedure is discussed at length in [12], to which we refer for details, while here we only recall some essential aspects. We assume $S_0 = 1$ and $q = 0$ throughout this section for simplicity. This normalization comes at no loss of generality, as the general case can be recovered simply replacing S_t with $S_0 S_t e^{qt}$ everywhere. Furthermore, let $t \in \mathbb{R}_+^\times$ be a fixed time horizon, and assume that $\mathbb{Q}(S_t > 0) = 1$ and that the law of $\log S_t$ with respect to \mathbb{Q} is absolutely continuous with a density belonging to L^2 .

Given constants $a \in \mathbb{R}_+^\times$ and $b \in \mathbb{R}$, define the random variable X by $aX + b = \log S_t$. The density f of the random variable X , that also belongs to L^2 , is then approximated by a finite linear combination of Hermite functions, the definition of which is recalled next. The Hermite polynomials $(H_n)_{n \geq 0}$ are defined by

$$H_n(x) := (-1)^n e^{x^2/2} \frac{d^n}{dx^n} e^{-x^2/2}, \quad n \in \mathbb{N}.$$

For instance, the first four of them are

$$H_0(x) = 1, \quad H_1(x) = x, \quad H_2(x) = x^2 - 1, \quad H_3(x) = x^3 - 3x.$$

The Hermite functions $(h_n)_{n \geq 0}$ are defined by

$$h_n(x) := H_n(\sqrt{2}x) e^{-x^2/2}.$$

Using well-known properties of Hermite polynomials, it is not hard to show that $\|h_n\|_{L^2}^2 = n! \sqrt{\pi} =: c_n$ for every $n \in \mathbb{N}$ and that $(h_n/c_n)_{n \in \mathbb{N}}$ is a complete orthonormal basis of L^2 . Therefore, setting, for every $n \in \mathbb{N}$,

$$\alpha_n := \frac{1}{n! \sqrt{\pi}} \langle f, h_n \rangle = \frac{1}{n! \sqrt{\pi}} \int_{\mathbb{R}} f(x) h_n(x) dx$$

and

$$f_n = \sum_{k=0}^n \alpha_k h_k,$$

one has $\lim_{n \rightarrow \infty} f_n = f$ in L^2 .

If $g: \mathbb{R}_+ \rightarrow \mathbb{R}$ is a measurable function such that $x \mapsto g(e^{ax+b})f(x) \in L^1$, or, equivalently, such that $\mathbb{Q}g(S_t)$ is finite, then the Hermite estimator of order n of

$$\mathbb{Q}g(S_t) = \int_{\mathbb{R}} g(e^{ax+b})f(x) dx$$

is

$$\int_{\mathbb{R}} g(e^{ax+b})f_n(x) dx = \sum_{k=0}^n \alpha_k \int_{\mathbb{R}} g(e^{ax+b})h_k(x) dx.$$

Remark 3.1. Since $f \in L^1 \cap L^2$ and the dual of $L^1 \cap L^2$ is $L^2 + L^\infty$, the assumption $x \mapsto g(e^{ax+b}) \in L^2 + L^\infty$ implies that $\mathbb{Q}g(S_t)$ is finite. However, this assumption is not sharp, as $g: x \mapsto x$ does not satisfy it, but $\mathbb{Q}S_t = 1$. The latter observation implies that Hermite estimators of call and put options are well defined.

The price at time zero of a put option with strike k is given by $\mathbb{Q}(\beta_t^{-1}k - S_t)^+$, which simplifies, assuming that r is nonrandom, to

$$\mathbb{Q}(ke^{-rt} - S_t)^+ = \int_{\mathbb{R}} (ke^{-rt} - e^{ax+b})^+ f(x) dx,$$

hence, setting

$$\zeta_+ := \frac{1}{a}(\log k - rt - b),$$

the Hermite estimator of the put option price is

$$ke^{-rt} \sum_{k=0}^n \alpha_k \int_{-\infty}^{\zeta_+} h_k(x) dx - \sum_{k=0}^n \alpha_k \int_{-\infty}^{\zeta_+} e^{ax+b} h_k(x) dx,$$

where both integrals can be computed explicitly in terms of the standard Gaussian cumulative distribution function Φ , or in terms of the [incomplete gamma function](#) (see [12] for details).

Once the Hermite estimators of put option prices have been defined, the coefficients (α_k) can be calibrated, for given constants a, b , to a set of observed put option prices in a very efficient way due to the linearity of the approximating price with respect to (α_k) . As a second step, calibration of the parameters a, b can also be performed in a numerically efficient way. Several calibration criteria and algorithms are discussed and tested empirically in [12]. Calibration is meant here and throughout the paper as minimization of a loss function applied to the absolute relative pricing error, defined as follows: if $\pi \in \mathbb{R}^N$ is a vector of observed prices of options with a fixed time to maturity and $\hat{\pi}(p) \in \mathbb{R}^N$ a the vector of option prices, with the same strike prices, depending on a parameter p , the vector of absolute relative pricing errors is $e = (e_1, \dots, e_N) \in \mathbb{R}^N$,

$$e_j := \left| \frac{\hat{\pi}_j}{\pi_j} - 1 \right| \quad \forall j = 1, \dots, N.$$

The loss function used to calibrate the Hermite estimator is the ℓ^2 norm (i.e. the Euclidean norm) to optimize with respect to $(\alpha)_k$ for given a, b , and the ℓ^1 norm to optimize with respect to a, b . Further aspects related to the construction of Hermite approximations will be discussed in §6.

4 A variance-gamma estimator

The variance-gamma estimator of option prices is constructed assuming that logarithmic returns follow a variance-gamma process with drift and calibrating its parameters to a set of observed data.

Let us first recall the basic definitions related to variance-gamma processes. The gamma measure on the Borel σ -algebra of \mathbb{R}_+ with parameters $c, \alpha \in \mathbb{R}_+^\times$, denoted by $\lambda_{c,\alpha}$, is defined by

$$\lambda_{c,\alpha}(A) := \frac{\alpha^c}{\Gamma(c)} \int_A x^{c-1} e^{-\alpha x} dx,$$

where $\Gamma(\cdot)$ denotes the **gamma function**. Let $c, \alpha \in \mathbb{R}_+^\times$. Since gamma measures are infinitely divisible, there exists a positive increasing Lévy process Γ with $\Gamma_0 = 0$ such that, for every $t \in \mathbb{R}_+$, the law of Γ_t is $\lambda_{ct,\alpha}$. We can now define variance-gamma processes as Wiener processes with drift subordinated to gamma processes. Let W be a standard Wiener process independent of Γ , and $\theta \in \mathbb{R}$, $\sigma \in \mathbb{R}_+^\times$. The stochastic process Y defined by

$$Y_t = \theta \Gamma_t + \sigma W_{\Gamma_t}$$

is a Lévy process called (asymmetric) variance-gamma process, that was introduced, at least in financial modeling, in [9], under the extra assumption that $c = \alpha$. We shall also use this simplification in our numerical work, but we continue the brief discussion in this section without assuming it. For every $t \in \mathbb{R}_+^\times$, the law of the random variable Y_t is absolutely continuous with a density that admits an explicit representation in terms of the **modified Bessel function of second kind** (this observation is also due to [9]), that can be written as

$$K_\nu(x) = \frac{1}{2}(x/2)^\nu \int_0^\infty t^{-\nu-1} \exp(-t - x^2/(4t)) dt$$

for $x \in \mathbb{R}$.

Lemma 4.1. *Let $t \in \mathbb{R}_+^\times$. The law of the random variable $\theta \Gamma_t + \sigma W_{\Gamma_t}$ is absolutely continuous with density*

$$\begin{aligned} f_{Y_t}(x) &= \int_0^\infty \frac{1}{\sigma\sqrt{s}} \phi\left(\frac{x - \theta s}{\sigma\sqrt{s}}\right) d\lambda_{ct,\alpha}(s) \\ &= \frac{2}{\sigma\sqrt{2\pi}} \frac{\alpha^{ct}}{\Gamma(ct)} \exp(x\theta/\sigma^2) \left(\frac{x^2}{\theta^2 + 2\alpha\sigma^2}\right)^{ct/2-1/4} K_{ct-1/2}\left(|x| \frac{\sqrt{\theta^2 + 2\alpha\sigma^2}}{\sigma^2}\right). \end{aligned}$$

A proof can be inferred from the one in [9].

In order to guarantee that the density (at a fixed time) of a variance-gamma process admits an expansion in Hermite functions, we need sufficient conditions for such density to be square integrable.

Proposition 4.2. *Let $t \in \mathbb{R}_+^\times$ be such that*

$$ct > \frac{1}{4}.$$

Then the density of Y_t belongs to L^2 .

The proof is a consequence of Minkowski's inequality applied to the first representation of the density of Y_t in Lemma 4.1. Details, as well as a more general result, will appear in [10]. It is not clear (to us) whether the condition is only sufficient or also necessary.

We can now discuss the modeling of financial returns by variance-gamma processes (with an additional drift term) and the corresponding pricing of European put options. We shall assume from now on that

$$\theta + \frac{\sigma^2}{2} < \alpha.$$

Setting

$$\eta = c \log \left(1 - \frac{\theta + \sigma^2/2}{\alpha} \right),$$

let us assume that the process S defined by

$$S_t = S_0 \exp(-qt + Y_t + \eta t)$$

is the discounted price process of an asset with constant dividend rate q with respect to a pricing measure \mathbb{Q} . A simple computation based on the tower property of conditional expectation and the moment generating function of gamma measures shows that S is a \mathbb{Q} -martingale.

Assuming that the short rate is nonrandom and equal to a constant r , the price at time zero of a European put option with strike price K and expiration time t on the asset with discounted price process S is given by

$$e^{-rt} \mathbb{Q} \left(K - S_0 \exp((r - q)t + \eta t + Y_t) \right)^+.$$

A more explicit expression can be obtained introducing the functions $\tilde{q}, \tilde{\sigma}: \mathbb{R}_+ \rightarrow \mathbb{R}$ defined by

$$\tilde{q}(x) := -(r - q + \eta)t - (\theta + \sigma^2/2)x, \quad \tilde{\sigma}(x) := \sigma\sqrt{x}.$$

Then, using the notation of §2, the price of the option is

$$e^{-rt} \mathbb{Q} \text{BS}(S_0, K, 0, \tilde{q}(\Gamma_t), \tilde{\sigma}(\Gamma_t), 1).$$

The computation of option prices is thus reduced to the computation of the expectation of a function of the gamma-distributed random variable Γ_t , that can be written as an integral. In fact, if $h: \mathbb{R}_+ \rightarrow \mathbb{R}$ is the function defined by

$$h(x) := e^{-rt} \text{BS}(S_0, K, 0, \tilde{q}(x), \tilde{\sigma}(x), 1),$$

then the price of the put option is given by

$$\int_0^\infty h(x) f_{\Gamma_t}(x) dx = \frac{\alpha^{ct}}{\Gamma(ct)} \int_0^\infty h(x) x^{ct-1} e^{-\alpha x} dx. \quad (4.1)$$

In the empirical work of later sections we shall use this formula, computing the integral numerically, to price options in the variance-gamma setting. Since a term in the integrand has a singularity at zero for $t < 1/c$, i.e. for options near expiration, the task is not entirely trivial. Some issues related to the numerical approximation of this type of integrals are discussed in [10].

Once a pricing formula for European options is available, calibration of the parameters is straightforward, at least theoretically: if $\pi \in \mathbb{R}^N$ is a vector of observed prices of options with a fixed time to maturity and $\hat{\pi}(\theta, \sigma, \alpha) \in \mathbb{R}^N$ is the vector of option prices, with the same strike prices, implied by a variance-gamma model with parameters θ , σ , and α , then we minimize the ℓ^1 norm of absolute relative pricing errors with respect to (θ, σ, α) . Note that, in contrast to the Hermite estimator, there is no linearity in any one of the parameters to calibrate. A few practical issues pertaining to the calibration of the variance-gamma estimator are discussed in the appendix.

5 A Heston estimator

In analogy to the previous section, the Heston estimator of option prices is constructed assuming that asset prices follow a so-called Heston stochastic volatility model, the parameters of which are calibrated to a set of observed option prices. This model is more “expensive” than the variance-gamma one, as it is specified by five rather than just three parameters.

We shall briefly recall the definition of the Heston model and establish an integrability result for the characteristic function of logarithmic returns, that will imply the square integrability of Heston densities. Under a pricing measure \mathbb{Q} , let $W = (W^1, W^2)$ be an \mathbb{R}^2 -valued Wiener process with covariance matrix

$$Q = \begin{bmatrix} 1 & \rho \\ \rho & 1 \end{bmatrix}, \quad \rho \in]-1, 1[,$$

and $S_0, v_0, \kappa, \theta, \eta \in \mathbb{R}_+^\times$ be such that the so-called Feller condition

$$2\kappa\theta > \eta^2$$

is satisfied. Then the system of stochastic differential equations

$$\begin{aligned} S_t &= S_0 - \int_0^t q S_s ds + \int_0^t \sqrt{v_s} S_s dW_s^1, \\ v_t &= v_0 + \int_0^t \kappa(\theta - v_s) ds + \int_0^t \eta \sqrt{v_s} dW_s^2 \end{aligned}$$

admits a unique solution, for which the Feller condition implies that $\mathbb{Q}(v_t > 0) = 1$ for every $t \geq 0$. Interpreting S as the discounted price process of an asset with constant dividend rate q and v as its squared volatility process, this model was introduced in [7] and is since then called the Heston (stochastic volatility) model. Note that the squared volatility v is a Feller square-root process, better known as Cox-Ingersoll-Ross process in the financial literature. The Heston model is hence a parametric model of asset prices with five parameters, namely $v_0, \kappa, \theta, \eta, \rho$, that admit the following interpretations: v_0 is the initial squared volatility; θ is the “equilibrium” (long-time) level of the squared volatility; κ is the rate of mean reversion of v towards its equilibrium level θ ; η is the volatility of volatility; ρ , as already mentioned, is just the correlation of the two driving Wiener processes.

A convenient technique to price options on assets with price process following a Heston model is via Fourier transform methods. In the following we shall assume, as done before, without loss of generality, that $q = 0$ and $S_0 = 1$. General results on affine processes (see, e.g., [4]), or the original arguments in [7]), imply that there exist functions $A, B: \mathbb{R} \times \mathbb{R}_+ \rightarrow \mathbb{C}$ such that the characteristic function ψ_t of $\log S_t$ can be written as

$$\psi_t(\xi) := \mathbb{Q} \exp(i\xi \log S_t) = \exp(A(\xi, t) + B(\xi, t)v_0).$$

Moreover, the functions A, B admit explicit expressions. Namely, introducing the functions $\alpha, \beta: \mathbb{R} \rightarrow \mathbb{C}$ defined by

$$\hat{\alpha}(\xi) := -\frac{1}{2}\xi(\xi + i), \quad \beta(\xi) := \kappa - i\eta\rho\xi,$$

setting $\gamma := \eta^2/2$, and introducing the functions $D, G: \mathbb{R} \rightarrow \mathbb{C}$ defined by

$$D := (\beta^2 - 4\gamma\hat{\alpha})^{1/2}, \quad G := \frac{\beta - D}{\beta + D},$$

one has

$$\begin{aligned} A(\xi, t) &:= \frac{\kappa\theta}{\eta^2} \left((\beta(\xi) + D(\xi))t - 2 \log \frac{e^{D(\xi)t} - G(\xi)}{1 - G(\xi)} \right), \\ B(\xi, t) &:= \frac{\beta(\xi) - D(\xi)}{\eta^2} \frac{1 - e^{-D(\xi)t}}{1 - G(\xi)e^{-D(\xi)t}}. \end{aligned}$$

In the expression for A the square root and the logarithm of a complex number $z = |z|(\cos \vartheta + i \sin \vartheta)$, $\vartheta \in [-\pi, \pi[$, are defined as

$$z^{1/2} := |z|^{1/2}(\cos \vartheta/2 + i \sin \vartheta/2), \quad \log z := \log|z| + i\vartheta$$

(the square root on the right-hand side of the first definition being in the sense of real numbers).

We shall need a criterion for the density of $\log S_t$ to belong to L^2 . The following lemma is just a technical step.

Lemma 5.1. *Let $\tilde{A}: \mathbb{R} \times \mathbb{R}_+ \rightarrow \mathbb{C}$ be the function defined by*

$$\tilde{A}(\xi, t) := \frac{\kappa\theta}{\eta^2} \left((\beta(\xi) - D(\xi))t - 2 \log \frac{G(\xi)e^{-D(\xi)t} - 1}{G(\xi) - 1} \right).$$

Then $\tilde{A} = A \bmod i\mathbb{R}$.

Proof. Writing $Dt = -Dt + 2Dt$, since $2Dt = -2 \log e^{-Dt} \bmod i\mathbb{R}$, one has

$$(\beta + D)t - 2 \log \frac{e^{Dt}/G - 1}{1/G - 1} = (\beta - D)t - 2 \log e^{-Dt} - 2 \log \frac{G - e^{Dt}}{G - 1} \quad \bmod i\mathbb{R},$$

where

$$\log e^{-Dt} + \log \frac{G - e^{Dt}}{G - 1} = \log \frac{Ge^{-Dt} - 1}{G - 1} \quad \bmod i\mathbb{R},$$

thus establishing the claim. \square

We can now establish an integrability property of the characteristic function ψ_t .

Proposition 5.2. *The characteristic function ψ_t of $\log S_t$ belongs to L^p for every $p \in [1, +\infty[$.*

Proof. By the **Riemann-Lebesgue lemma**, ψ_t is uniformly continuous and null at infinity, in particular it is bounded. Therefore it is enough to show that ψ_t is p -integrable outside an arbitrarily large compact set. In view of Lemma 5.1, the functions A and \tilde{A} differ only by an imaginary term, hence it suffices to show that $\exp(\tilde{A} + B) = \exp \tilde{A} \exp B$ belongs to L^p . Setting $c := \kappa\theta/\eta^2$ for convenience, one has

$$\exp(\tilde{A}(\xi, t)) = \left(\frac{G(\xi) - 1}{G(\xi)e^{-D(\xi)t} - 1} \right)^{2c} \exp(c(\beta(\xi) - D(\xi))t).$$

Since

$$\begin{aligned} \beta^2 - 4\gamma\hat{\alpha} &= (\kappa - i\eta\rho\xi)^2 + \eta^2\xi(\xi + i) \\ &= \kappa^2 + (1 - \rho^2)\eta^2\xi^2 + i\eta(\eta - 2\kappa\rho)\xi, \end{aligned}$$

with $|\rho| < 1$, the real part of $\beta^2 - 4\gamma\hat{\alpha}$ is positive. This in turn implies that the real part of $(\beta^2 - 4\gamma\hat{\alpha})^{1/2}$ is positive. More precisely, setting $\beta^2 - 4\gamma\hat{\alpha} =: z =: |z|e^{i\vartheta}$, one has

$$\begin{aligned} |z|^{1/2} &= (\kappa^4 + 2\kappa^2(1 - \rho)^2\eta^2\xi^2 + (1 - \rho^2)^2\eta^4\xi^4 + \eta^4(\eta - 2\kappa\rho)^4\xi^4)^{1/4}, \\ \vartheta &= \arctan \frac{\eta(\eta - 2\kappa\rho)\xi}{\kappa^2 + (1 - \rho^2)\eta^2\xi^2}, \end{aligned}$$

hence $(\beta^2 - 4\gamma\hat{\alpha})^{1/2} = |z|^{1/2}e^{i\vartheta/2}$. Since $\lim_{\xi \rightarrow \infty} \vartheta(\xi) = 0$, there exists $\xi_0 \in \mathbb{R}_+$ such that, for every $\xi \in \mathbb{R}$ with $|\xi| > \xi_0$,

$$\operatorname{Re}(\beta(\xi) - D(\xi)) \approx 1 - |\xi|.$$

Let us now show that the function $G - 1$ is bounded. In fact,

$$|G(\xi) - 1| = 2 \frac{|D(\xi)|}{|\beta(\xi) + D(\xi)|},$$

where $|D(\xi)|^2 \approx 1 + \xi^2$ and

$$\beta(\xi) + D(\xi) = \kappa - i\eta\rho\xi + |z|^{1/2}(\cos \vartheta/2 + i \sin \vartheta/2),$$

where, entirely similarly as above, $|z|^{1/2}(\xi) \approx 1 + |\xi|$ for $|\xi|$ sufficiently large, and $\lim_{\xi \rightarrow \infty} \vartheta(\xi) = 0$, from which it immediately follows that $|\beta(\xi) + D(\xi)| \approx 1 + |\xi|$ for ξ outside a compact set. Therefore the function $G - 1$, as well as G itself, are bounded outside a compact set. Since the real part of $D(\xi)$, as seen above, is proportional to $1 + |\xi|$ for $|\xi|$ large, this also implies that

$$\lim_{\xi \rightarrow \infty} |G(\xi)e^{-D(\xi)t}| = 0,$$

thus also that

$$\lim_{\xi \rightarrow \infty} |G(\xi)e^{-D(\xi)t} - 1| = 1,$$

from which it follows that the function $(G - 1)/(Ge^{-Dt} - 1)$ is bounded outside a compact set. Therefore $\operatorname{Re} \exp A(\xi, t) \approx \exp(c(1 - |\xi|))$ for every ξ outside a compact set. Concerning B , note that, thanks to the previous estimates,

$$\lim_{\xi \rightarrow \infty} \frac{1 - e^{-D(\xi)t}}{1 - G(\xi)e^{-D(\xi)t}} = 1,$$

hence, recalling that $\operatorname{Re}(\beta(\xi) - D(\xi)) \approx 1 - |\xi|$ for $|\xi|$ large, it follows that $\operatorname{Re} B(\xi, t) \approx 1 - |\xi|$ outside a compact set. We have thus shown that, for ξ outside a compact set, there exists a strictly positive constant C such that $\psi_t(\xi) \approx \exp(-C|\xi|)$, which implies that $\psi_t \in L^p$ for every $p \in [1, +\infty]$. \square

Corollary 5.3. *The density of the random variable $\log S_t$ belongs to L^2 .*

Proof. Immediate recalling that the Fourier transform is an (isometric) isomorphism of L^2 . \square

As the characteristic function of $\log S_t$ is known, prices of put options can be efficiently computed by an approach, by now classical, apparently first proposed in [3]. In particular, denoting the logarithm of the strike price by k and the law of the random variable $\log S_t$ by μ , the price of a put option with strike price e^k can be written as

$$p(k) := \int_{-\infty}^k (e^k - e^x) d\mu(x),$$

for which it is easily seen that, for any $\alpha \leq -1$, the function p_α defined by

$$p_\alpha(k) := e^{\alpha k} p(k),$$

belongs to L^1 . Therefore, introducing the Fourier transform of p_α defined by

$$\mathcal{F}p_\alpha(\xi) := \int_{\mathbb{R}} e^{-2i\pi\xi k} p_\alpha(k) dk,$$

if $\mathcal{F}p_\alpha \in L^1$, then, by inverse Fourier transform, one has, using well-known properties of Fourier transforms of real-valued functions,

$$\begin{aligned} p(k) &= e^{-\alpha k} p_\alpha(k) = e^{-\alpha k} \int_{\mathbb{R}} e^{2i\pi\xi k} \mathcal{F}p_\alpha(\xi) d\xi \\ &= 2e^{-\alpha k} \int_0^\infty e^{2i\pi\xi k} \mathcal{F}p_\alpha(\xi) d\xi \\ &= 2e^{-\alpha k} \int_0^\infty \operatorname{Re} e^{2i\pi\xi k} \mathcal{F}p_\alpha(\xi) d\xi. \end{aligned}$$

A simple computation based on Tonelli's theorem yields

$$\mathcal{F}p_\alpha(\xi) = \frac{\mathcal{F}\mu(\xi + i(\alpha + 1)/(2\pi))}{(\alpha + 1 - i2\pi\xi)(\alpha - i2\pi\xi)},$$

therefore, setting

$$\psi(\xi, \alpha) := \operatorname{Re} \frac{\mathcal{F}\mu(\xi + i(\alpha + 1)/(2\pi))}{(\alpha + 1 - i2\pi\xi)(\alpha - i2\pi\xi)}$$

for convenience of notation, one has

$$p(k) = 2e^{-\alpha k} \int_0^\infty \psi(\xi, \alpha) d\xi.$$

Even though the right-hand side does not depend on α , the choice of α influences the accuracy of numerical integration. We shall adopt the methods of [8], selecting α in an automated payoff-dependent way (cf. [8, p. 13, eq. (60)]), reducing the integral over \mathbb{R}_+ to an integral over a finite domain thanks to precise asymptotic relations for the function ψ , for which we refer to [8, Proposition 2.2].

Calibration of Heston models to observed option prices is done, *mutatis mutandis*, as already described at the end of §4. Some related numerical issues are discussed in the appendix.

6 Hermite approximation of densities

Before looking at the empirical performance of variance-gamma and Heston estimators compared with some Hermite estimators with the same number of parameters, it seems interesting, as a preliminary step, to examine whether variance-gamma and Heston densities can be approximated by truncated expansions in Hermite functions, how good the approximations are in L^2 norm, and whether Hermite approximations can estimate option prices implied by the parametric densities within reasonable error bounds. While numerical experiments are deferred to §§7.1-7.2, in §6.1 we discuss some issues regarding expansions in series of Hermite functions of arbitrary densities of logarithmic returns, showing that optimizing the scale and location parameters is feasible and that some classes of constrained Hermite approximations can be computed explicitly from unconstrained ones. In §§6.2-6.3 we deal with the computation of the coefficients (α_k) of Hermite approximations to variance-gamma and Heston densities, respectively, showing that in the former case the (α_k) admit closed-form expressions in terms of integrals with respect to gamma measures, while in the latter case they can be written as the scalar product in L^2 of Hermite functions and a simple modification of the Fourier transform of the density.

6.1 Densities of logarithmic returns

According to the usual conventions, let S_t denote the discounted price of an asset at time t . We shall assume, for the purposes of this subsection, that t is fixed, $q = 0$, $S_0 = 1$, $\mathbb{Q}(S_t > 0) = 1$, and that the law of $\log S_t$ with respect to \mathbb{Q} admits a density f belonging to L^2 .

Since f belongs to L^2 , given an orthonormal basis (h_n) of L^2 , one can always write $f = \sum_{n \in \mathbb{N}} \alpha_n h_n$, with $\alpha_n := \langle f, h_n \rangle$ and the identity to be understood in the L^2 sense. If (h_n) are (properly scaled) Hermite functions, a truncation of the series representing f provides a finite-dimensional approximation that, however, turns out to be too crude for the purposes of estimating option prices. It is instead much preferable to formally set $\log S_t = aX + b$, for some constants a, b (the choice of which will be discussed next) and a random variable X , and to approximate the density of X , rather than the density of $\log S_t$. Since the density of X is easily seen to be $x \mapsto af(ax + b)$, setting $f_{a,b}: x \mapsto f(ax + b)$ and

$$\alpha_k := \alpha_k(a, b) := \frac{1}{\|h_k\|_{L^2}^2} \langle f_{a,b}, h_k \rangle = \frac{1}{k! \sqrt{\pi}} \langle f_{a,b}, h_k \rangle \quad \forall k \in \mathbb{N},$$

so that

$$f_{a,b} = \sum_{k=0}^{\infty} \alpha_k h_k$$

as an identity in L^2 , one has

$$a \int_{\mathbb{R}} \left| f(ax+b) - \sum_{k=0}^{\infty} \alpha_k h_k(x) \right|^2 dx = \int_{\mathbb{R}} \left| f(x) - \sum_{k=0}^{\infty} \alpha_k h_k\left(\frac{x-b}{a}\right) \right|^2 dx,$$

from which it is immediate that, for every $n \in \mathbb{N}$, one can approximate the density of $\log S_t$, in the L^2 sense, by the function f_n defined by

$$f_n(x) := \sum_{k=0}^n \alpha_k h_k\left(\frac{x-b}{a}\right),$$

that is the projection of f on the finite-dimensional subspace of L^2 spanned by the functions $(h_k((\cdot - b)/a))_{k=0, \dots, n}$.

Let us consider the issue of choosing the constants a and b . As already mentioned (cf. also [12]), if one interprets the Hermite approximation of the density of X as a perturbation of the Black-Scholes model for asset prices, in the sense that the Hermite approximation of order zero coincides with the Black-Scholes model, for which $\log S_t = \zeta Z - \zeta^2/2$ in law, with Z standard Gaussian random variable and $\zeta \in \mathbb{R}_+^\times$, then the constant a and b would have to be chosen as

$$b = -a^2/2, \quad b = \mathbb{Q} \log S_t,$$

or, alternatively, as

$$b = \mathbb{Q} \log S_t, \quad a = \text{Std}_{\mathbb{Q}} \log S_t := (\mathbb{Q}(\log S_t - b)^2)^{1/2}.$$

Note that these two choices of the constants a and b are equivalent if $\log S_t = \zeta Z - \zeta^2/2$, but are in general *not* equivalent. Moreover, the martingale property of S and Jensen's inequality imply that $\mathbb{Q} \log S_t \leq 0$, so there is no issue with the former choice of constants. On the other hand, in order for the standard deviation of $\log S_t$ to be well defined, it is necessary to assume that $\mathbb{Q}(\log S_t)^2 < \infty$ or, equivalently, $\int_{\mathbb{R}} x^2 f(x) dx < \infty$. This condition is automatically satisfied if, for instance, f is symmetric, as in this case

$$\int_{\mathbb{R}} x^2 f(x) dx = 2 \int_{\mathbb{R}_+} x^2 f(x) dx \leq 2 \int_{\mathbb{R}_+} e^x f(x) dx \leq 2 \mathbb{Q} S_t = 2.$$

It is also easy to check that

$$\int x^2 f_n(x) dx < \infty \quad \forall n \in \mathbb{N}.$$

A further natural step is to select the constants a and b by an optimization procedure, i.e., setting

$$f_n^{s,m} := \sum_{k=0}^n \alpha_k(s,m) h_k((\cdot - m)/s)$$

for convenience of notation, and $J(s,m) := \|f - f_n^{s,m}\|_{L^2}^2$, to consider the problem

$$\inf_{(s,m) \in \mathbb{R}_+^\times \times \mathbb{R}} J(s,m)$$

and, assuming that a minimizer (m_*, s_*) exist, to set $a := s_*$ and $b := m_*$. For the minimization of J it is useful to show that it is smooth, which we do next. We start with a simple bound that is going to be used often.

Lemma 6.1. *Let $A_1 \subset \mathbb{R}_+^\times$, $A_2, A_3 \subset \mathbb{R}$ be compact sets, $A := A_1 \times A_2 \times A_3$, and $(P_i)_{i \in I}$ be an arbitrary collection of polynomials of degree bounded by $n \in \mathbb{N}$, such that their coefficients belong to A_3 . There exists a function $g: \mathbb{R} \rightarrow \mathbb{R}_+$, belonging to L^p for every $p \in [1, \infty]$, such that, for every $x \in \mathbb{R}$, $i \in I$, $a \in A_1$, and $b \in A_2$, one has*

$$\left| P_i(x) \phi\left(\frac{x-a}{b}\right) \right| \lesssim_{n,A} g(x).$$

Proof. Let $i \in I$. The polynomial P_i is the sum of monomials $c_k x^k$, where $k \in \mathbb{N}$, $k \leq n$, hence $|x|^k \leq 1 + |x|^n$ for all $x \in \mathbb{R}$, and there exists $c \in \mathbb{R}_+^\times$ such that $|c_k| \leq c$. Then $|P_i(x)| \leq cn(1 + |x|^n)$. Moreover, setting $a_* := \max_{a \in A_1} |a|$ and $b_* := \max_{b \in A_2} |b|$, one has, for every $x \in \mathbb{R}$,

$$-\frac{1}{2} \frac{(x-b)^2}{a^2} \leq -\frac{1}{2} \frac{b^2 - 2bx + x^2}{a_*^2}$$

which implies

$$\exp\left(-\frac{1}{2} \frac{(x-b)^2}{a^2}\right) \leq \exp(-b^2/(2a_*^2)) \exp(bx/a_*^2) \exp(-x^2/(2a_*^2)),$$

where the first term on the right hand side is bounded by a constant depending only on A , and the second is bounded by $\exp(b_*|x|/a_*^2)$. Therefore, defining the function g by

$$g(x) := \exp(-x^2/(2a_*^2) + b_*|x|/a_*^2)(1 + |x|^n),$$

that is easily seen to belong to L^p for every $p \in [1, \infty]$, it follows that $|f_n| \lesssim g$ pointwise with an implicit constant depending only on n and A , as claimed. \square

Corollary 6.2. *Let $s_0, s_1, m_0 \in \mathbb{R}_+^\times$ with $s_0 < s_1$. There exists a function $g: \mathbb{R} \rightarrow \mathbb{R}_+$, belonging to L^p for every $p \in [1, \infty]$, such that, for every $x \in \mathbb{R}$, $s \in [s_0, s_1]$, and $m \in [-m_0, m_0]$, one has*

$$|f_n^{s,m}(x)| \lesssim g(x) \quad \forall x \in \mathbb{R},$$

where the implicit constant depends only on n , s_0 , m_0 , and $\|f\|_{L^2}$.

Proof. In the identity

$$f_n^{s,m}(x) = \sqrt{2\pi} \sum_{k=0}^n \alpha_k(s, m) H_k\left(\frac{x-m}{s}\right) \phi\left(\frac{x-m}{s}\right)$$

one has, by the Cauchy-Schwarz inequality, that, for every $k \leq n$,

$$|\alpha_k(s, m)| = |\langle f(s \cdot + m), h_k \rangle| \leq \|f(s \cdot + m)\|_{L^2} \|h_k\|_{L^2} = \frac{\sqrt{k! \sqrt{\pi}}}{\sqrt{s}} \|f\|_{L^2},$$

i.e. $|\alpha_k|$ is bounded by a constant depending on n , s_0 , and $\|f\|_{L^2}$. Moreover, for every $k \leq n$, $H_k((x-m)/s)$ is a polynomial of degree k and coefficients of the type m^p/s^q , with $p, q \in \mathbb{N}$. Since $m^p/s^q \leq m_0^p/s_0^q$, it immediately follows that

$$\sum_{k=0}^n \alpha_k(s, m) H_k\left(\frac{x-m}{s}\right)$$

is a polynomial in x with coefficients that are uniformly bounded by a constant depending on n , s_0 , m_0 , and $\|f\|_{L^2}$. The claim then follows by Lemma 6.1. \square

Lemma 6.3. For any $k \in \mathbb{N}$, the function

$$\begin{aligned} \mathbb{R}_+^\times \times \mathbb{R} &\longrightarrow L^2 \\ (s, m) &\longmapsto h_k\left(\frac{\cdot - m}{s}\right) \end{aligned}$$

is of class C^∞ .

Proof. The function $s \mapsto (x - m)/s$ is of class C^∞ for every $x, m \in \mathbb{R}$ and the function $m \mapsto (x - m)/s$ is of class C^∞ for every $x \in \mathbb{R}$ and every $s \in \mathbb{R}_+^\times$. Since H_k and ϕ are both of class C^∞ , it follows by composition that $(s, m) \mapsto h_k((x - m)/s)$ are of class C^∞ for every $x \in \mathbb{R}$. Therefore, if (s_n, m_n) is a sequence in $\mathbb{R}_+^\times \times \mathbb{R}$ converging to (s, m) , this implies, thanks to Corollary 6.2 and the dominated convergence theorem, that

$$\lim_{n \rightarrow \infty} \int_{\mathbb{R}} |h_k((x - m_n)/s_n) - h_k((x - m)/s)|^2 dx = 0,$$

i.e. that the function $(s, m) \mapsto h_k((\cdot - m)/s)$ is continuous. Moreover, the function $s \mapsto h_k((x - m)/s)$ is differentiable for every $x \in \mathbb{R}$ with derivative

$$s \mapsto -\frac{1}{s^2}(x - m)h'_k\left(\frac{x - m}{s}\right),$$

that is

$$\lim_{h \rightarrow 0} \frac{1}{h} (h_k((x - m)/(s + h)) - h_k((x - m)/s)) + \frac{1}{s^2}(x - m)h'_k((x - m)/s) = 0$$

for every $x \in \mathbb{R}$. The fundamental theorem of calculus yields

$$h_k((x - m)/(s + h)) - h_k((x - m)/s) = \int_0^h \frac{1}{(s + t)^2}(x - m)h'_k((x - m)/(s + t)) dt,$$

where, by Lemma 6.1, for h sufficiently small the absolute value of the integrand on the right-hand side is bounded uniformly with respect to t by an L^2 function g (of x), so that

$$\frac{1}{h} |h_k((x - m)/(s + h)) - h_k((x - m)/s)| \leq \frac{1}{h} \int_0^h g(x) dt = g(x).$$

The dominated convergence theorem then allows to conclude that

$$\lim_{h \rightarrow 0} \int_{\mathbb{R}} \left| \frac{1}{h} (h_k((x - m)/(s + h)) - h_k((x - m)/s)) + \frac{1}{s^2}(x - m)h'_k((x - m)/s) \right|^2 dx = 0,$$

thus proving that $s \mapsto h_k((\cdot - m)/s)$ is differentiable with derivative

$$s \mapsto -\frac{1}{s^2}(\cdot - m)h'_k((\cdot - m)/s).$$

Entirely similar (in fact slightly simpler) arguments show that $m \mapsto h_k((\cdot - m)/s)$ is differentiable with derivative

$$m \mapsto -\frac{1}{s}h'_k((\cdot - m)/s).$$

A further application of Lemma 6.1 shows that the partial derivatives of the function $(s, m) \mapsto h_k((\cdot - m)/s)$ are continuous, hence that the function is Fréchet differentiable and of class C^1 . Moreover, the function $(s, m) \mapsto h_k((x - m)/s)$ has continuous partial derivatives of every order for every $x \in \mathbb{R}$ that can be written as a polynomial (with coefficients given by continuous functions of m and $1/s$) multiplied by the density function of Gaussian random variable with mean m and standard deviation s , from which it follows, by repeated applications of Lemma 6.1 and the dominated convergence theorem, that $(s, m) \mapsto h_k((\cdot - m)/s): \mathbb{R}^2 \rightarrow L^2$ admits continuous partial derivatives of every order, hence that it is of class C^∞ . \square

Remark 6.4. Continuity of $(s, m) \mapsto h_k((\cdot - m)/s)$ can be proved in at least two other ways: in the first way as a consequence of the more general result according to which translations and dilations are strongly continuous linear operators on L^p for every $p \in [1, \infty[$. The second way proceeds noting that

$$\|h_k((\cdot - m)/s)\|_{L^2} = \sqrt{s}\|h_k\|_{L^2}$$

immediately implies that $(s, m) \mapsto \|h_k((\cdot - m)/s)\|_{L^2}$ is continuous and bounded on every bounded subset of $\mathbb{R}_+^\times \times \mathbb{R}$. The **Brezis-Lieb lemma** (see [2]) then easily yields that $(s, m) \mapsto h_k((\cdot - m)/s)$ is continuous from $\mathbb{R}_+^\times \times \mathbb{R}$ to L^2 .

Proposition 6.5. *For any $n \in \mathbb{N}$, the function*

$$\begin{aligned} \mathbb{R}_+^\times \times \mathbb{R} &\longrightarrow L^2 \\ (s, m) &\longmapsto f_n^{s,m} = \sum_{k=0}^n \alpha_k(s, m) h_k\left(\frac{\cdot - m}{s}\right) \end{aligned}$$

is of class C^∞ .

Proof. For any $k \in \mathbb{N}$,

$$\alpha_k(s, m) = \langle f(s \cdot + m), h_k \rangle = \frac{1}{s} \langle f, h_k((\cdot - m)/s) \rangle,$$

where, by Lemma 6.3, $(s, m) \mapsto h_k((\cdot - m)/s) \in C^\infty(\mathbb{R}^2; L^2)$. Since the map $\langle f, \cdot \rangle: L^2 \rightarrow \mathbb{R}$ is linear and continuous, hence of class C^∞ , it follows immediately, by composition, that $(s, m) \mapsto \alpha_k(s, m) \in C^\infty(\mathbb{R}^2)$. Therefore, since the product $\mathbb{R} \times L^2 \rightarrow L^2$ is bilinear and continuous, hence smooth, one has

$$(s, m) \mapsto \alpha_k(s, m) h_k((\cdot - m)/s) \in C^\infty(\mathbb{R}^2; L^2)$$

for every $k \in \mathbb{N}$, from which the claim follows immediately. \square

Proposition 6.6. *The function $J: \mathbb{R}_+^\times \times \mathbb{R} \rightarrow \mathbb{R}$ is of class C^∞ .*

Proof. The function J is the composition of $(s, m) \mapsto f_n^{s,m} - f \in C^\infty(\mathbb{R}^2; L^2)$ and $\|\cdot\|_{L^2}^2 \in C^\infty(L^2)$, hence $J \in C^\infty(\mathbb{R}^2)$. \square

Let us compute the derivatives of first and second order of J . As a first step, note that, for any $g \in L^2$, $D\|g\|_{L^2}^2 = v \mapsto 2\langle g, v \rangle$, hence, by the chain rule for (Fréchet derivatives), $DJ = 2\langle f - f_n, Df_n \rangle$. For the purposes of this computation only, let us denote the function $(s, m) \mapsto h_k((\cdot - m)/s): \mathbb{R}^2 \rightarrow L^2$ also by h_k . Denoting the canonical basis of \mathbb{R}^2 by (e_1, e_2) , one has, as in the proof of Lemma 6.3,

$$\begin{aligned} [Dh_k]e_1 &= (s, m) \mapsto \partial_1 h_k((\cdot - m)/s) = -\frac{1}{s^2}(\cdot - m)h'_k((\cdot - m)/s) \\ [Dh_k]e_2 &= (s, m) \mapsto \partial_2 h_k((\cdot - m)/s) = -\frac{1}{s}h'_k((\cdot - m)/s), \end{aligned}$$

hence $Dh_k: \mathbb{R}_+^\times \times \mathbb{R} \rightarrow \mathcal{L}(\mathbb{R}^2; L^2)$ is identified (by linearity) by the above expressions for $[Dh_k]e_1$ and $[Dh_k]e_2$. Similarly,

$$\begin{aligned} \partial_1 \alpha_k &: (s, m) \mapsto -\frac{1}{k! \sqrt{\pi}} \frac{1}{s^2} \langle f, h_k((\cdot - m)/s) \rangle - \frac{1}{k! \sqrt{\pi}} \frac{1}{s^3} \langle f, (\cdot - m)h'_k((\cdot - m)/s) \rangle, \\ \partial_2 \alpha_k &: (s, m) \mapsto -\frac{1}{k! \sqrt{\pi}} \frac{1}{s^2} \langle f, h'_k((\cdot - m)/s) \rangle \end{aligned}$$

hence $D\alpha_k: \mathbb{R}^2 \rightarrow \mathcal{L}(\mathbb{R}^2; \mathbb{R}) \simeq \mathbb{R}^2$ is identified, thanks to linearity, by $[D\alpha_k]e_1 = \partial_1\alpha_k$ and $[D\alpha_k]e_2 = \partial_2\alpha_k$. Then $D(\alpha_k h_k) = h_k D\alpha_k + \alpha_k Dh_k$, where h_k is interpreted as a function $\mathbb{R}^2 \rightarrow \mathcal{L}(\mathbb{R}; L^2)$, hence

$$Df_n = \sum_{k=0}^n h_k D\alpha_k + \alpha_k Dh_k: \mathbb{R}_+^\times \times \mathbb{R} \longrightarrow \mathcal{L}(\mathbb{R}^2; L^2)$$

and DJ is identified by

$$[DJ]e_i = 2\langle f - f_n, [Df_n]e_i \rangle, \quad i = 1, 2.$$

In order to compute D^2J , recall that $(g_1, g_2) \mapsto \langle g_1, g_2 \rangle: L^2 \times L^2 \rightarrow \mathbb{R}$ is, as every continuous bilinear map, continuously differentiable, with Fréchet derivative $D\langle g_1, g_2 \rangle: (h, k) \mapsto \langle g_1, k \rangle + \langle g_2, h \rangle$. Then, by the chain rule,

$$D^2J = D(f - f_n, Df_n): \mathbb{R}^2 \rightarrow \mathcal{L}(\mathbb{R}^2; \mathcal{L}(\mathbb{R}^2; L^2)) \simeq \mathcal{L}_2(\mathbb{R}^2; L^2)$$

is the function with values in the space of symmetric bilinear forms on \mathbb{R}^2 with values in L^2 defined, for every $u, v \in \mathbb{R}^2$, by

$$(u, v) \mapsto -\langle [Df_n]u, [Df_n]v \rangle + \langle f - f_n, [D^2f_n](u, v) \rangle.$$

An explicit expression for $[D^2f_n](u, v)$ can be obtained as follows:

$$[D^2(\alpha_k h_k)](u, v) = D\alpha_k(u) Dh_k(v) + D\alpha_k(v) Dh_k(u) + D^2\alpha_k(u, v) h_k + \alpha_k D^2h_k(u, v),$$

where, considering \mathbb{R}^2 with its canonical basis, $D^2\alpha_k$ and D^2h_k are represented by their Hessian matrices (with real and L^2 -valued entries, respectively).

Even though the objective function J is (infinitely many times) differentiable with respect to its arguments, with explicit expressions for its derivatives, it does not seem simple to determine analytically whether minimizers exist and, if they do, to identify global minima. In practice, one relies on numerical minimization algorithms using as initial values for s and m the values of a and b discussed above. This procedure can be interpreted as locally optimizing the constants in a Hermite perturbation of a starting Gaussian (i.e. Black-Scholes) approximation of logarithmic returns. Note that the availability of easily implementable expressions for the gradient of the objective function, that follows from the above results, can speed up numerical minimization algorithms considerably. Since second derivatives are easily implementable as well, it is also possible to check numerically in an efficient way whether critical points for the gradient are (local) minimum points.

We are now going to discuss a class of Hermite approximations subjects to constraints. As motivation, note that the function f_n is not, in general, the density of a random variable, as it may assume negative values and may not have unit integral. While enforcing a positivity constraint on Hermite approximations such as f_n seems unfeasible, it is relatively simple to determine, for fixed a and b , the best L^2 approximation of f of the type

$$\tilde{f}_n(x) = \sum_{k=0}^n \beta_k h_k \left(\frac{x-b}{a} \right),$$

with (β_k) constants, such that

$$\int_{\mathbb{R}} \tilde{f}_n(x) dx = 1.$$

In geometric terms, the problem amounts to finding the projection of f on the finite-dimensional closed convex subset of L^2 formed by functions such as \tilde{f}_n . This projection can be characterized explicitly and is a consequence of the next more general fact.

Let $L \in \text{Hom}(\mathbb{R}^{n+1}; \mathbb{R}^m)$ be surjective (in particular, $m \leq n+1$), $v \in \mathbb{R}^m$, and $H := \{\beta \in \mathbb{R}^{n+1} : L\beta = v\}$. The matrix representing the homomorphism L with respect to the canonical bases of \mathbb{R}^{n+1} and \mathbb{R}^m will be denoted by L as well.

Lemma 6.7. *Let $\alpha \in \mathbb{R}^{n+1}$. The problem*

$$\inf_{\beta \in H} \|\beta - \alpha\|_{\mathbb{R}^{n+1}}$$

admits a solution and the infimum is attained by the vector

$$\beta_* := \alpha - L^\top (LL^\top)^{-1} (L\alpha - v).$$

Proof. Consider the Lagrangian

$$F(\beta; \lambda) := \frac{1}{2} \|\beta - \alpha\|_{\mathbb{R}^{n+1}}^2 + \langle \lambda, L\beta - v \rangle_{\mathbb{R}^m}$$

where λ is a \mathbb{R}^m -valued Lagrange multiplier. The Fréchet derivative of $\beta \mapsto F(\beta; \lambda)$ is given, in matrix notation, by

$$D_\beta F(\beta; \lambda) = \beta - \alpha + L^\top \lambda.$$

Setting $D_\beta F(\beta; \lambda)$ equal to zero yields $\beta(\lambda) := \alpha - L^\top \lambda$. Enforcing the constraint defining H implies

$$v = L\beta = L\alpha - LL^\top \lambda,$$

where LL^\top is invertible because L has full rank. Therefore, setting

$$\lambda_* = (LL^\top)^{-1} (L\alpha - v)$$

and

$$\beta_* := \beta(\lambda_*) = \alpha - L^\top (LL^\top)^{-1} (L\alpha - v),$$

it follows easily that β_* is the unique minimizer. \square

For notational convenience, let $h_k^{a,b}$ denote the function $h_k((\cdot - b)/a)$. Let V_n denote the subspace of L^2 spanned by $\{h_0^{a,b}, \dots, h_n^{a,b}\}$, and

$$C_n := \left\{ \sum_{k=0}^n \alpha_k h_k^{a,b} : \alpha := (\alpha_0, \dots, \alpha_n) \in \mathbb{R}^{n+1}, L\alpha = v \right\}.$$

It is clear that V_n is isomorphic to \mathbb{R}^{n+1} and C_n is a (closed) convex subset of V_n . We need to introduce some notation that is only needed because $(h_k^{a,b})$ is an orthogonal basis of L^2 , but not orthonormal. We shall set, for all $k \in \mathbb{N}$,

$$\check{\alpha}_k := \alpha_k \|h_k^{a,b}\|_{L^2}, \quad \hat{h}_k^{a,b} := \frac{h_k^{a,b}}{\|h_k^{a,b}\|_{L^2}},$$

and similarly for other quantities. Moreover, the matrix $\hat{L} = (\hat{l}_{ij})$ is defined by

$$\hat{l}_{ij} := \frac{l_{ij}}{\|h_k^{a,b}\|_{L^2}}.$$

Then $(\hat{\psi}_k^{a,b})$ is an orthonormal basis of L^2 , if $f = \sum_{k=0}^\infty \alpha_k h_k^{a,b}$ then $f = \sum_{k=0}^\infty \check{\alpha}_k \hat{h}_k^{a,b}$, and the constraint $L\alpha = v$ is equivalent to $\hat{L}\check{\alpha} = v$.

Proposition 6.8. *Let $f \in L^2$, (α_k) the set of coefficients of its expansion with respect to the orthogonal basis of L^2 formed by $(h_k^{a,b})$,*

$$\check{\beta} := \check{\alpha} - \hat{L}^\top (\hat{L}\hat{L}^\top)^{-1} (\hat{L}\check{\alpha} - v),$$

and

$$\beta_k := \frac{\check{\beta}_k}{\|h_k^{a,b}\|_{L^2}} \quad \forall k = 1, \dots, n.$$

Then the projection of $f \in L^2$ onto the convex set C_n is given by

$$\tilde{f}_n := \sum_{k=0}^n \beta_k h_k^{a,b}.$$

Proof. It is clear that $\tilde{f}_n \in C_n$, so it is enough to show that $\|f - \tilde{f}_n\| \leq \|f - g\|$ for every $g \in C_n$. Suppose, by contradiction, that there exists $\gamma \in \mathbb{R}^{n+1}$ such that, setting $g := \sum \gamma_k h_k^{a,b}$,

$$\|f - g\|_{L^2} < \|f - \tilde{f}_n\|_{L^2}.$$

The inequality is equivalent to

$$\begin{aligned} & \left\| \sum_{k=0}^n (\check{\alpha}_k - \check{\gamma}_k) \hat{h}_k^{a,b} + \sum_{k=n+1}^{\infty} \check{\alpha}_k \hat{h}_k^{a,b} \right\|_{L^2}^2 \\ & < \left\| \sum_{k=0}^n (\check{\alpha}_k - \check{\beta}_k) \hat{h}_k^{a,b} + \sum_{k=n+1}^{\infty} \check{\alpha}_k \hat{h}_k^{a,b} \right\|_{L^2}^2. \end{aligned}$$

Therefore, by orthonormality,

$$\|\check{\alpha} - \check{\gamma}\|_{\mathbb{R}^{n+1}} = \sum_{k=0}^n (\check{\alpha}_k - \check{\gamma}_k)^2 < \sum_{k=0}^n (\check{\alpha}_k - \check{\beta}_k)^2 = \|\check{\alpha} - \check{\beta}\|_{\mathbb{R}^{n+1}},$$

which contradicts the optimality of $\check{\beta}$, hence is impossible. \square

It is now clear that Proposition 6.8 gives the solution to the problem of finding the best approximation in L^2 of f among the linear combinations of Hermite functions with unit integral. Explicit formulas for the coefficients of L (which reduces to a vector in this case) can be found in [12]. One may also add as further constraint for the approximation \tilde{f}_n to satisfy the property

$$\int_{\mathbb{R}} e^{ax+b} \tilde{f}_n(x) dx = 1, \quad (6.1)$$

that can be seen as an approximate martingale condition. Also in this case explicit expressions for the corresponding matrix L are available in [12].

Once the desired, possibly constrained, approximation of f has been obtained, it is easy to compute the L^2 error. One has

$$\left\| f - \sum_{k=0}^n \beta_k h_k^{a,b} \right\|_{L^2}^2 = \|f\|_{L^2}^2 + \sum_{k=0}^n \beta_k^2 \|h_k^{a,b}\|_{L^2}^2 - 2 \sum_{k=0}^n \beta_k \langle f, h_k^{a,b} \rangle,$$

where $\|h_k^{a,b}\|_{L^2}^2 = a \|h_k\|_{L^2}^2$ and $\langle f, h_k^{a,b} \rangle = a \|h_k\|_{L^2}^2 \alpha_k$, hence

$$\left\| f - \sum_{k=0}^n \beta_k h_k^{a,b} \right\|_{L^2}^2 = \|f\|_{L^2}^2 + a \left(\sum_{k=0}^n \beta_k^2 \|h_k\|_{L^2}^2 - 2 \sum_{k=0}^n \alpha_k \beta_k \|h_k\|_{L^2}^2 \right).$$

If $\beta_k = \alpha_k$ for all k , i.e. in the unconstrained case, the squared L^2 error simplifies to

$$\|f\|_{L^2}^2 - a \sum_{k=0}^n \alpha_k^2 \|h_k\|_{L^2}^2.$$

Finally, recall that $\|h_k\|_{L^2}^2 = \sqrt{\pi} k!$.

Remark 6.9. The approximation f_n is specified by $n + 3$ parameters, namely by the $n + 1$ coefficients (α_k) and the parameters a, b . Constrained approximations of the type discussed above reduce the dimensionality by the number of independent constraints, hence the so-called approximate martingale approximation is specified by $n + 3 - 2 = n + 1$ parameters, as the constraints of having unit integral and integrating $x \mapsto e^{ax+b}$ to one are independent (cf. [12]).

6.2 Variance-gamma densities

Let us consider the Hermite approximation, in the sense of §6.1, of the density of a variance-gamma process X of the type $X_t = \theta\Gamma_t + \sigma W_{\Gamma_t} + \eta t$, as defined in §4, so that, in particular, the process $\exp X$ is a \mathbb{Q} -martingale. Let Y be the process defined by $Y_t := \theta\Gamma_t + \sigma W_{\Gamma_t}$ and, for a fixed $t \in \mathbb{R}_+^\times$, denote the density of Y_t by f . Then the density of X_t is

$$f(x - \eta t) = \int_0^\infty \frac{1}{\sigma\sqrt{s}} \phi\left(\frac{x - \eta t - \theta\sqrt{s}}{\sigma\sqrt{s}}\right) d\lambda_{ct, \alpha}(s).$$

If $ct > 1/4$, which implies that f , hence also $f(\cdot - \eta t)$, belong to L^2 , then, setting

$$\alpha_k = \frac{1}{k!\sqrt{\pi}} \int_{\mathbb{R}} f(ax + b - \eta t) h_k(x) dx,$$

one has, as an identity in L^2 ,

$$f(x - \eta t) = \sum_{k=0}^{\infty} \alpha_k h_k\left(\frac{x - b}{a}\right).$$

Since the density f admits an explicit expression (in terms of special functions), the numerical computation of (α_k) is easy to implement. The computation of (α_k) can also be written as an integral with respect to a gamma measure: as a first step, note that, by Fubini's theorem,

$$\begin{aligned} \alpha_k &\simeq_k \int_{\mathbb{R}} f(ax + b - \eta t) h_k(x) dx \\ &\simeq \int_{\mathbb{R}} \int_{\mathbb{R}_+} \frac{1}{\sigma\sqrt{s}} \phi\left(\frac{x - \eta t - \theta\sqrt{s}}{\sigma\sqrt{s}}\right) d\lambda_{ct, \alpha}(s) H_k\left(\sqrt{2}\frac{x - b}{a}\right) \phi\left(\frac{x - b}{a}\right) dx \\ &= \int_{\mathbb{R}_+} \frac{1}{\sigma\sqrt{s}} \int_{\mathbb{R}} H_k\left(\sqrt{2}\frac{x - b}{a}\right) \phi\left(\frac{x - b}{a}\right) \phi\left(\frac{x - \eta t - \theta\sqrt{s}}{\sigma\sqrt{s}}\right) dx d\lambda_{ct, \alpha}(s). \end{aligned}$$

To continue we need an analytic lemma, the proof of which is elementary, hence omitted.

Lemma 6.10. *Let $\mu_1, \mu_2 \in \mathbb{R}$, $\sigma_1, \sigma_2 \in \mathbb{R}_+^\times$, and*

$$\begin{aligned} \mu &:= \mu_1 \frac{\sigma_2^2}{\sigma_1^2 + \sigma_2^2} + \mu_2 \frac{\sigma_1^2}{\sigma_1^2 + \sigma_2^2}, \\ \sigma &:= \frac{\sigma_1 \sigma_2}{\sqrt{\sigma_1^2 + \sigma_2^2}}, \\ c &:= \frac{1}{\sigma^2} \left(\frac{\mu_1^2}{\sigma_1^2} + \frac{\mu_2^2}{\sigma_2^2} - \mu^2 \right). \end{aligned}$$

Then

$$\phi\left(\frac{x - \mu_1}{\sigma_1}\right) \phi\left(\frac{x - \mu_2}{\sigma_2}\right) = \frac{1}{\sqrt{2\pi}} \phi\left(\frac{x - \mu}{\sigma}\right) \exp c.$$

Therefore there exist functions $c, m, \varsigma: \mathbb{R}_+ \rightarrow \mathbb{R}$, depending on the parameters a, b, θ, σ , such that

$$\phi\left(\frac{x - b}{a}\right) \phi\left(\frac{x - \eta t - \theta\sqrt{s}}{\sigma\sqrt{s}}\right) = e^{c(s)} \phi\left(\frac{x - m(s)}{\varsigma(s)}\right),$$

hence the inner integral in the above expression for α_k can be written as

$$e^c \int_{\mathbb{R}} H_k \left(\frac{x-b}{a/\sqrt{2}} \right) \phi \left(\frac{x-m}{\varsigma} \right) dx = \varsigma e^c \int_{\mathbb{R}} H_k \left(\frac{\varsigma x + m - b}{a/\sqrt{2}} \right) \phi(x) dx,$$

where the integral on the right-hand side can be reduced to computing integrals of the type

$$\int_{\mathbb{R}} x^h e^{-x^2/2} dx, \quad h \in \mathbb{N},$$

that admit explicit expressions in terms of the gamma function. We have thus shown that the function

$$F(s) := \int_{\mathbb{R}} H_k \left(\sqrt{2} \frac{x-b}{a} \right) \phi \left(\frac{x-b}{a} \right) \phi \left(\frac{x - \eta t - \theta \sqrt{s}}{\sigma \sqrt{s}} \right) dx$$

can be written in terms of explicit functions (among which we include the gamma function), hence that α_k is obtained as the integral of F with respect to the gamma measure $\lambda_{ct,\alpha}$.

6.3 Heston densities

Let S be the discounted price process in a Heston stochastic volatility model, as introduced in §5, with the normalizing assumptions $q = 1$ and $S_0 = 1$, and let a strictly positive time t be fixed. Assuming that the coefficients satisfy the Feller condition, S_t is strictly positive with probability one and, by Corollary 5.3, $\log S_t$ admits a density $f \in L^2$. Even though an explicit expression for the density f is not available, the coefficients (α_k) of the Hermite approximation of f can be written as integrals involving the characteristic function ψ_t of $\log S_t$, for which explicit forms are known, and the Hermite functions h_k , thanks to general properties of the Fourier transform.

If $g \in L^1$, let us define its Fourier transform \widehat{g} by

$$\widehat{g}(\xi) := \frac{1}{\sqrt{2\pi}} \int_{\mathbb{R}} g(x) e^{-ix\xi} dx.$$

The same notation will be used for the usual extension of the Fourier transform to L^2 . Moreover, recall that the Fourier transform is a unitary operator of L^2 , i.e., for any $g, h \in L^2$,

$$\langle g, h \rangle = \langle \overline{\widehat{g}}, \widehat{h} \rangle,$$

where $\overline{}$ stands for complex conjugation.

Proposition 6.11. *Let $a \in \mathbb{R}_+^\times$, $b \in \mathbb{R}$, $\psi_{a,b}: \mathbb{R} \rightarrow \mathbb{C}$ the function defined by*

$$\psi_{a,b}(\xi) := \frac{e^{-ib\xi/a}}{a} \psi_t(\xi/a),$$

and, for each $k \in \mathbb{N}$,

$$\alpha_k := \begin{cases} \frac{(-1)^{k/2}}{\pi k! \sqrt{2}} \langle \operatorname{Re} \psi_{a,b}, h_k \rangle, & \text{if } k \in 2\mathbb{N}, \\ \frac{(-1)^{k/2+3/2}}{\pi k! \sqrt{2}} \langle \operatorname{Im} \psi_{a,b}, h_k \rangle, & \text{if } k \in 2\mathbb{N} + 1, \end{cases}$$

Then the following identity holds in L^2 :

$$f = \sum_{k=0}^{\infty} \alpha_k h_k \left(\frac{\cdot - b}{a} \right).$$

Proof. It follows immediately from $f \in L^2$ that $f_{a,b} \in L^2$, hence, as $h_k \in L^2$ as well,

$$\langle f_{a,b}, h_k \rangle = \langle \widehat{f_{a,b}}, \widehat{h_k} \rangle,$$

where, by well-known properties of the Fourier transform,

$$\widehat{f_{ab}}(\xi) = \frac{e^{ib\xi/a}}{a} \widehat{f}(\xi/a).$$

Moreover, **Hermite functions are eigenfunctions of the Fourier transform**, with

$$\widehat{h_k}(\xi) = (-i)^k h_k(\xi) \quad \forall k \in \mathbb{N}.$$

Since f is real, hence so is $f_{a,b}$, one has

$$\overline{\widehat{f_{a,b}}(\xi)} = \widehat{f_{a,b}}(-\xi)$$

and, by definition of characteristic function (suppressing the index t for simplicity),

$$\widehat{f}(\xi) = \frac{1}{\sqrt{2\pi}} \psi(-\xi),$$

hence

$$\overline{\widehat{f_{a,b}}(\xi)} = \frac{1}{a} \overline{e^{ib\xi/a} \widehat{f}(\xi/a)} = \frac{e^{-ib\xi/a}}{a} \overline{\widehat{f}(\xi/a)} = \frac{e^{-ib\xi/a}}{a\sqrt{2\pi}} \psi(\xi/a).$$

Recalling the definition of $\psi_{a,b}$, the above yields, after some algebraic manipulations,

$$\langle f_{a,b}, h_k \rangle = \frac{(-i)^k}{\sqrt{2\pi}} \langle \psi_{a,b}, h_k \rangle = \begin{cases} \frac{(-1)^{k/2}}{\sqrt{2\pi}} \langle \operatorname{Re} \psi_{a,b}, h_k \rangle, & \text{if } k \in 2\mathbb{N}, \\ \frac{(-1)^{k+(k+1)/2}}{\sqrt{2\pi}} \langle \operatorname{Im} \psi_{a,b}, h_k \rangle, & \text{if } k \in 2\mathbb{N} + 1, \end{cases}$$

from which the claim follows immediately, recalling that $\alpha_k = \langle f_{a,b}, h_k \rangle / (k! \sqrt{\pi})$. \square

7 Empirical results

Approximations of variance-gamma and Heston densities are investigated empirically in this section. As a first step we look at approximations by Hermite methods of variance-gamma and Heston densities, in the sense discussed in §6, in two test cases. We shall see that, as far as the variance-gamma density is concerned, that is determined by three parameters, estimates by Hermite approximations with the same number of parameters seem rather poor. On the other hand, Hermite approximations depending on five parameters of a Heston density, that depends on the same number of parameters, appear to be quite precise in terms of their L^2 distance from the target, although their pricing accuracy is not consistently satisfying. Moreover, we conduct an extensive empirical analysis on a sample of put option prices on the S&P500 index for the whole year 2012.¹ Namely, we compare the empirical performance of variance-gamma and Heston option price estimators (in the sense of out-of-sample estimates) against several classes of Hermite estimators depending on three and five free parameters, respectively.

¹Only options with low trading volumes or that violated price monotonicity with respect to strike prices were discarded. After these adjustments, the dataset included 43 469 contracts. The most active day was December 21 (the 242nd day), with 269 put prices across 14 expiration dates.

7.1 Hermite approximation of variance-gamma densities

7.1.1 A synthetic example

We first consider, as an example, a variance-gamma process Y with parameters

$$\theta = 0.1, \quad \sigma = 0.3, \quad \alpha = 2,$$

and we approximate the density f of its drifted version X , defined by $X_t = Y_t + \eta t$, evaluated at $t = 1$, where the notation of §4 is used throughout. The random variable $X_t = X_1$ can be interpreted as $\log S_t$, where S is a martingale discounted price process of an asset, assuming no dividends for simplicity. The mean and standard deviation of the density f are -0.0505 and 0.308 , respectively, while its L^2 norm is 1.01 .

In the notation and terminology of §6.1, we are going to consider four types of Hermite estimators, all depending on the same number of free parameters as the variance-gamma distribution, i.e. three. The simplest one assumes the parameters a and b to satisfy $b = -a^2/2$, with b equal to the mean of X_t , and to have two (unconstrained) Hermite coefficients α_0, α_1 . As already mentioned in §6.1, the resulting approximation of f , denoted by $f_{1,p}$, can be interpreted as a perturbation of the Black-Scholes model (hence the subscript p). The refinement of this approximation obtained by optimizing with respect to the constant a is denoted by $f_{1,p}^*$. Just to fix notation, we set, for every $n \in \mathbb{N}$,

$$f_{n,p}(x) = \sum_{k=0}^n \alpha_k h_k((x + a^2/2)/a),$$

and $f_{n,p}^*$ will stand for its optimized version (with respect to a). If the parameters a, b are chosen in terms of the density and standard deviation of f as above, the Hermite approximation of order three with the coefficients (α_k) satisfying the so-called approximate martingale property has three free parameters, and is thus another natural candidate to approximate the variance-gamma density. Denoting the generic Hermite approximation of order $n \in \mathbb{N}$ satisfying the approximate martingale property by $f_{n,m}$ and its optimized version (with respect to the parameter a) by $f_{n,m}^*$, we are thus going to consider $f_{3,m}$ and $f_{3,m}^*$. In the next subsection on the Hermite approximation of Heston densities we shall also discuss approximations f_n with independent parameters a, b , but we do not consider them here. The reason is that these approximations are characterized by $n + 3$ parameters, hence we would have to take $n = 0$ to have three parameters, but the f_0 approximation is degenerate and is just proportional to a Gaussian density.

The distance from f of $f_{1,p}$, $f_{3,m}$, and of their starred versions in the sense of the L^2 , L^1 , and L^∞ norms, expressed in percentage of the corresponding norm of f , are collected in Table 1. As can easily be inferred from the reported values (cf. also Figure 1), approximation errors

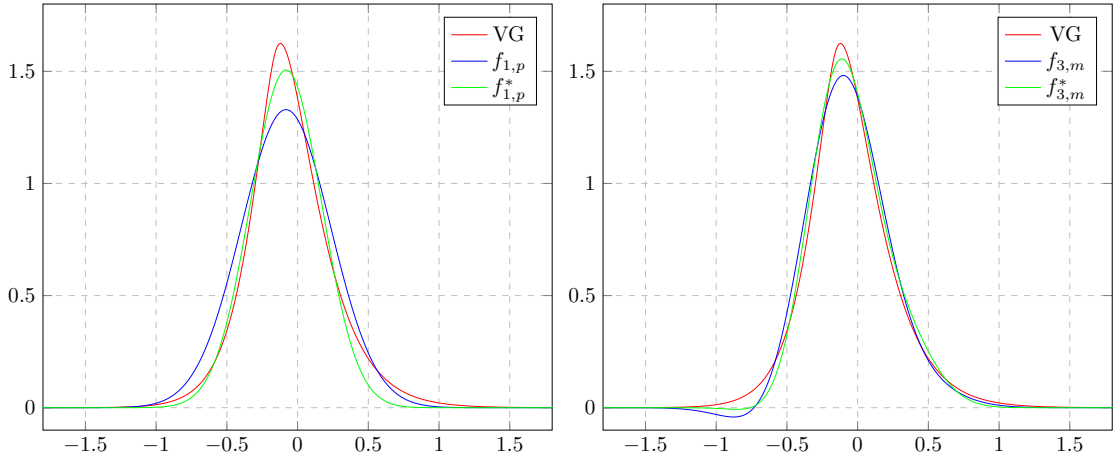
Table 1: Hermite Approximation Error of a Test Variance-Gamma Density

For all $g \in \{f_{1,p}, f_{1,p}^*, f_{3,m}, f_{3,m}^*\}$ and $q \in \{1, 2, \infty\}$, the relative error $\|f - g\|_{L^q} / \|f\|_{L^q}$ in percentage points is reported, where f is the test variance-gamma density.

Norm	$f_{1,p}$	$f_{1,p}^*$	$f_{3,m}$	$f_{3,m}^*$
L^2	17.6	9.87	10.4	7.39
L^1	19.7	12.4	12.6	9.64
L^∞	19.0	9.25	10.1	5.14

appear too large to be useful for the purpose of approximating integrals against f by integrals against any one of its approximations, as would be the case in option pricing. However, it is at the same time remarkable that a function defined in terms of the standard deviation of f and

Figure 1: Hermite approximations of a test variance-gamma (VG) density



two Hermite polynomials, hence a largely uninformed device, can “explain” 90% of the L^2 norm of f . The relative L^∞ error achieved by the $f_{3,m}^*$ is also remarkable.

To investigate how the various approximation schemes perform as estimators of option prices, we proceed as follows: let K_1, \dots, K_N be strike prices randomly sampled from a uniform distribution on $[1/2, 5/4]$ with $N = 20$. Variance-gamma prices of put options with this set of strike prices can then be computed. That is, assuming that the underlying is an asset with discounted price process modeled by $S = \exp X$, i.e. by a variance-gamma dynamics with the parameters introduced at the beginning of the subsection, corresponding put option prices are obtained. Each approximation of f produces an estimate of the variance-gamma prices of the put options, e.g. $f_{1,p}$ determines the approximation

$$\int_{\mathbb{R}} (K_i - e^x)^+ f_{1,p}(x) dx, \quad i = 1, \dots, N.$$

The absolute relative pricing error (an element of $[0, 1]^N$) for each of the proposed approximations is then determined, and descriptive statistics are collected in Table 2. It turns out that, in spite of the relatively poor approximations of f achieved by the Hermite approximations, the option price estimator associated to $f_{1,p}^*$ obtains quite good results, with 75% of the price estimates within 3.54% of the target variance-gamma price.

We also consider “corrected” option prices, in the sense of (2.1), where we assume that the variance-gamma price of the put option with strike price k_0 is known. Of course this reduces the size of the sample from N to $N - 1$. For simplicity, we take k_0 equal to the median of the N strike prices K_1, \dots, K_N . Descriptive statistics of the absolute relative error in percentage points are collected in Table 3. In this case, apart from the $f_{3,m}$ estimator, that is consistently off target, all estimators perform reasonably well, with occasional very large errors compromising their average error in some cases. In particular, the $f_{1,p}^*$ and $f_{3,m}^*$ estimators stand out, with 75% of their price estimates within 4.17% and 0.533% of the target price, respectively.

Lastly, we address a different but related question: given the above set of option prices generated by a variance-gamma model, does a Hermite option price estimator calibrated to these prices display acceptable accuracy? Numerical results suggest that calibrating to option prices an approximation to f of the type $f_{1,p}$ (this calibration was called H_σ in [12]) produces quite satisfying results, with mean relative pricing error equal to 4.67%, and quantiles at 75% and 95% level equal to 4.32% and 14.7%, respectively.

Table 2: Absolute Relative Pricing Errors by Hermite Approximations of a Test Variance-Gamma Density

For a set of twenty randomly generated strike prices in the interval $[0.5, 1.25]$, descriptive statistics on the absolute relative error of put option prices generated by the approximations $\{f_{1,p}, f_{1,p}^*, f_{3,m}, f_{3,m}^*\}$ with respect to the put option prices generated by the test variance-gamma density f are reported (all data in percentage points).

MEAN				
	$f_{1,p}$	$f_{1,p}^*$	$f_{3,m}$	$f_{3,m}^*$
	33.0	8.17	100	20.8

DISTRIBUTION				
Quantile	$f_{1,p}$	$f_{1,p}^*$	$f_{3,m}$	$f_{3,m}^*$
25%	14.0	2.17	100	5.88
50%	31.2	2.84	100	12.1
75%	43.3	3.54	100	18.0
95%	74.1	45.9	100	82.1
99%	74.7	67.1	100	100

7.1.2 One day of real data

As a next step, we consider one day of real data (day 242 of our dataset), made up by several blocks of options having the same time to maturity. The parameters of a variance-gamma density are then calibrated to each block, minimizing the mean absolute relative pricing error. Errors and values of the calibrated parameters for each block are displayed in Table 4. For each block, we approximate the calibrated variance-gamma density using the Hermite schemes introduced above, and compute their estimation errors in terms of the norms L^2 , L^1 , and L^∞ (except for the first three blocks, for which the condition for the density to be in L^2 is not satisfied). The L^2 estimation errors in the remaining nine blocks range between 28% and 62%, thus making the corresponding approximations of very limited use. The calibration of Hermite estimators to the option prices corresponding to the calibrated variance-gamma models unfortunately produces comparable results, leading to the conclusion that Hermite approximation of variance-gamma densities and of option prices generated by such densities may not be satisfactory, at least not when the Hermite approximation schemes depend only on three free parameters.

7.2 Hermite approximation of Heston densities

7.2.1 A synthetic example

As an example we consider, in the notation of §5, the density f at time $t = 1$ of $\log S_t$, assuming $S_0 = 1$, $q = 0$, and the parameters

$$v_0 = 0.05, \quad \kappa = 1, \quad \theta = 0.1, \quad \eta = 0.25, \quad \rho = -0.75,$$

that satisfy the Feller condition. The density f has mean and standard deviation equal to -0.0342 and 0.271 , respectively, and its L^2 norm is 1.11 .

In analogy to the discussion in §7.1, we consider Hermite approximations of f that depends on the same number of parameters specifying the Heston density, that is five. The simplest

Table 3: Absolute Relative Pricing Errors by Hermite Approximations of a Test Variance-Gamma Density (“Corrected” Prices)

For the same set of twenty randomly generated strike prices in the interval $[0.5, 1.25]$ as in Table 2, descriptive statistics on the absolute relative error of put option prices generated by the approximations $f_{1,p}, f_{1,p}^*, f_{3,m}, f_{3,m}^*$ with respect to the “corrected” put option prices, in the sense of (2.1), generated by the test variance-gamma density f are reported (all data in percentage points).

MEAN				
	$f_{1,p}$	$f_{1,p}^*$	$f_{3,m}$	$f_{3,m}^*$
	18.0	2.57	91.3	17.1

DISTRIBUTION				
Quantile	$f_{1,p}$	$f_{1,p}^*$	$f_{3,m}$	$f_{3,m}^*$
25%	0.124	0.586	100	0.276
50%	0.343	0.837	100	0.462
75%	4.17	1.00	100	0.533
95%	100	16.7	100	100
99%	100	24.8	100	100

Hermite approximation is thus $f_{3,p}$, defined by

$$f_{3,p}(x) = \sum_{k=0}^3 \alpha_k h_k((x + a^2/2)/a),$$

where the parameter b is equal to the mean of $\log S_t$ and a is such that $b = -a^2/2$. The refined approximation $f_{3,p}^*$ obtained by optimizing with respect to the parameter a is also employed. The relative L^2 , L^1 , and L^∞ errors in the approximation of f are reported in the first two columns of Table 5. Both approximations appear to be satisfactory: the L^2 and L^∞ do not exceed approximately 3.5%, while the L^1 error of $f_{3,p}$ is approximately 4.7%, improving to 4.1% for $f_{3,p}^*$. Moreover, note that the improvement in the approximation caused by the optimization with respect to the parameter a is significant but not dramatic. This observation confirms that interpreting Hermite approximations as perturbations of the Black-Scholes model is at least meaningful. As a further Hermite approximation of f depending on five parameters, we consider the approximation of order two with unconstrained constants a and b , that is, in the notation §6.1, f_2 , as well as its refinement f_2^* obtained by optimizing with respect to a and b . The approximation errors of these two schemes (see the third and fourth columns of Table 5) are much higher than those attained by $f_{3,p}$ and $f_{3,p}^*$, suggesting that it is not efficient to swap a location-scale parameter with an order of Hermite expansion. Moreover, even though the optimized approximation f_2^* is much better than the approximation f_2 , the former assumes negative values on a non-negligible portion of the right tail, which is certainly an undesirable feature. The last pair of Hermite approximations we consider is composed of $f_{5,m}$ and $f_{5,m}^*$. Recall that the former is obtained constraining the Hermite coefficients (α_k) of f_5 , with $b = -a^2/2$, to satisfy the so-called approximate martingale property, and the latter is its optimized version (with respect to a). The approximation errors are collected in the last two columns of Table 5. While the approximation $f_{5,m}$ has essentially the same L^2 error of $f_{3,p}^*$, but significantly higher L^1 and L^∞ errors also than those of the more elementary $f_{3,p}$, the optimized approximation $f_{5,m}^*$ has significantly lower errors than all other approximations, with an impressive relative L^∞ error of

Table 4: Variance-Gamma Calibration on One Day of Data

Mean absolute relative pricing error for each block of day 242 of the dataset. Each row corresponds to a block and contains the time to maturity in days, the error in percentage points, and the values of the calibrated parameters.

Maturity	Error	θ	σ	α
4	21.4	-0.0743	0.147	0.743
10	15.2	-0.0910	0.175	2.800
13	15.5	-0.0667	0.180	2.980
17	3.61	-0.0209	0.177	8.590
24	2.37	-0.0046	0.175	6.610
32	6.55	-0.0405	0.161	3.760
60	3.65	0.0292	0.193	2.330
88	3.61	-0.0562	0.176	2.510
186	11.0	-0.1670	0.134	1.660
277	0.332	0.0667	0.234	0.788
368	0.888	-0.2020	0.078	1.040
732	15.4	-0.1400	0.090	0.272

Table 5: Hermite Approximation Errors of a Test Heston Density

For all $g \in \{f_{3,p}, f_{3,p}^*, f_2, f_2^*, f_{5,m}, f_{5,m}^*\}$ and $q \in \{1, 2, \infty\}$, the relative error $\|f - g\|_{L^q} / \|f\|_{L^q}$ in percentage points is reported, where f is the test Heston density.

Norm	$f_{3,p}$	$f_{3,p}^*$	f_2	f_2^*	$f_{5,m}$	$f_{5,m}^*$
L^2	3.53	3.08	12.2	7.17	3.07	2.60
L^1	4.68	4.10	15.6	10.5	6.04	3.55
L^∞	3.35	2.83	11.2	5.18	6.63	1.62

1.62% (cf. Figure 2).

The good accuracy of several approximations of f introduced thus far in terms of L^2 (as well as L^1 and L^∞) norms does not necessarily translate in good estimates of option prices. Moreover, if g_1, g_2 are approximations of f and the distance of g_1 from f is less than the distance of g_2 from f in any one of the above norms, it does not follow that approximate option prices computed replacing f by g_1 are better than those computed replacing f by g_2 . Therefore, in analogy to what we have done in §7.1, we consider the same set K_1, \dots, K_N of strike prices, for which prices of put options are computed assuming that the underlying is an asset with discounted asset price modeled by S , i.e. by a Heston dynamics with the parameters introduced at the beginning of the subsection. These Heston prices are then compared to the price estimates produced by each one of the Hermite approximations considered above. The mean absolute relative pricing errors and quantiles of their empirical distributions are reported in Table 6. The basic $f_{3,p}$ approximation, that, we recall, can be interpreted as a perturbation of the Black-Scholes model, clearly outperforms all other approximations, and appears to be a good estimator of Heston option prices, with all relative errors not exceeding 3%. It is interesting to observe that the optimized approximation $f_{3,p}^*$ performs much worse than its basic version, and that the $f_{5,m}$ approximation is completely off target, while its optimized version performs reasonably well, but

Figure 2: Hermite approximations of a test Heston density

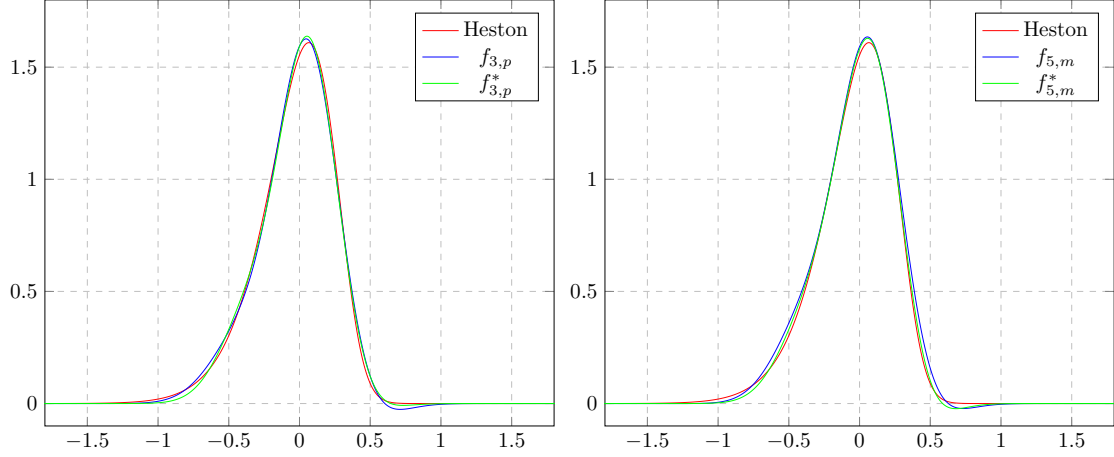


Table 6: Errors of Hermite Estimates of Synthetic Heston Prices

For the same set of twenty randomly generated strike prices in the interval $[0.5, 1.25]$ as in Table 2, descriptive statistics on the absolute relative error of put option prices generated by the approximations $\{f_{3,p}, f_{3,p}^*, f_2, f_2^*, f_{5,m}, f_{5,m}^*\}$ with respect to the put option prices generated by the test Heston density f are reported (all data in percentage points).

MEAN						
	$f_{3,p}$	$f_{3,p}^*$	f_2	f_2^*	$f_{5,m}$	$f_{5,m}^*$
	0.62	4.95	20.5	17.2	73.0	4.02

DISTRIBUTION						
Quantile	$f_{3,p}$	$f_{3,p}^*$	f_2	f_2^*	$f_{5,m}$	$f_{5,m}^*$
25%	0.0523	2.91	12.1	10.5	75.3	1.84
50%	0.382	3.58	14.7	12.7	84.2	2.77
75%	1.05	7.55	32.6	26.9	94.2	6.42
95%	2.06	10.9	45.7	37.1	95.8	10.3
99%	2.92	13.1	53.0	42.8	96.2	12.7

Table 7: Absolute Relative Pricing Errors by Hermite Approximations of a Test Heston Density (“Corrected” Prices)

For the same set of twenty randomly generated strike prices in the interval $[0.5, 1.25]$ as in Table 2, descriptive statistics on the absolute relative error of put option prices generated by the approximations $f_{3,p}$, $f_{3,p}^*$, f_2 , f_2^* , $f_{5,m}$, $f_{5,m}^*$ with respect to the “corrected” put option prices, in the sense of (2.1), generated by the test Heston density f are reported (all data in percentage points).

MEAN						
	$f_{3,p}$	$f_{3,p}^*$	f_2	f_2^*	$f_{5,m}$	$f_{5,m}^*$
	0.270	0.729	7.09	6.41	81.3	0.187

DISTRIBUTION						
Quantile	$f_{3,p}$	$f_{3,p}^*$	f_2	f_2^*	$f_{5,m}$	$f_{5,m}^*$
25%	0.140	0.218	0.779	1.17	38.2	0.00215
50%	0.308	0.284	1.09	1.34	77.2	0.176
75%	0.337	0.658	1.98	2.16	100	0.371
95%	0.729	4.32	52.1	44.4	100	0.425
99%	1.04	5.78	53.7	46.4	100	0.435

still considerably worse than the more elementary $f_{3,p}$ approximation. Hence the added level of sophistication of $f_{5,m}^*$ may not be worth the effort, at least as far as the problem of estimating the price of a limited set of put options is concerned. Moreover, the rule of thumb according to which swapping a Hermite function for a degree of freedom in the choice of parameters a, b is inefficient is confirmed by these data.

Considering the price of the put option with the median strike price as observed, hence known, and applying (2.1), we obtain “corrected” Hermite price estimates, for which we table mean absolute relative error and quantiles of its empirical distribution in Table 7. While the overall good accuracy of $f_{3,p}$ is confirmed, the picture regarding $f_{5,m}^*$, with a relative pricing error not exceeding approximately 0.44%, improves drastically, suggesting that, under the realistic assumption that a “true” option price is available, the added level of sophistication of $f_{5,m}^*$ compared to the more elementary $f_{3,p}$ may indeed pay off.

To conclude the analysis, we investigate how Hermite price estimators calibrated to the above set of Heston option prices perform. We shall only consider a Hermite estimator of the type $f_{3,p}$, about which the numerical results suggest that it matches the Heston prices with a relative pricing error that is essentially negligible: the mean absolute relative error is 0.0538%, the median error is 0.0397%, and the largest error is 0.179%. While it is clear that calibrating a Heston estimator to observed prices must produce better estimates than going through a direct approximation of the density f (simply by looking at the objective functions of the two procedures), the achieved accuracy is nonetheless remarkable. One should also mention that the calibration of a Hermite estimator of put option prices does not “care” about the density of the underlying on the set $[\log K_{\max}, +\infty[$, where K_{\max} is the largest strike price in the set of observed options. In this sense, the task of calibrating a Hermite price estimator to a set of put options is less demanding than approximating a density. Of course the same remark would apply, *mutatis mutandis*, to a set of call options.

Table 8: Heston Calibration on One Day of Data

Mean absolute relative pricing error for each block of day 242 of the dataset. Each row corresponds to a block and contains the time to maturity in days, the error in percentage points, and the values of the calibrated parameters.

Maturity	Error	v_0	θ	ρ	κ	η
4	51.7	0.000435	3.94	-0.984	0.71	2.37
10	31.6	0.000542	0.125	-0.979	14.2	1.88
13	26.5	1.55E-09	0.518	-0.982	2.24	1.52
17	5.29	0.0024	0.0822	-0.966	11.7	1.39
24	4.78	0.00266	0.192	-0.925	3.17	1.1
32	14.7	1.79E-07	0.175	-0.971	2.94	1.01
60	10.3	0.00211	0.162	-0.941	1.83	0.769
88	7.02	0.00693	2.05	-0.854	0.0813	0.577
186	11.6	0.00144	0.14	-0.918	1.02	0.533
277	20.1	0.0181	1.13	0.929	0.0723	2.78E-05
368	0.773	0.00205	0.141	-0.935	0.681	0.438
732	19.7	0.00206	0.356	-0.952	0.163	0.341

Table 9: Hermite Approximation Errors of Calibrated Heston Densities in One Day of Real Data

For all $g \in \{f_{3,p}, f_{3,p}^*, f_{5,m}, f_{5,m}^*\}$ and $q \in \{1, 2, \infty\}$, the average relative error $\|f - g\|_{L^q} / \|f\|_{L^q}$ in percentage points is reported, where f is the calibrated Heston density for each block of day 242. The average is taken over all blocks.

Norm	$f_{3,p}$	$f_{3,p}^*$	$f_{5,m}$	$f_{5,m}^*$
L^2	26.4	15.6	23.5	15.1
L^1	35.1	23.2	32.2	22.3
L^∞	27.3	14.3	23.8	13.0

7.2.2 One day of real data

We are now going to consider issues analogous to those treated in the previous paragraph when applied to the data pertaining to day 242 of our dataset. A Heston density is calibrated to each block, minimizing the ℓ^1 norm of relative pricing errors. The estimated Heston parameters for each block, see Table 8, display some patterns: the initial value of the squared volatility v_0 is close to zero; the long-term equilibrium level θ of the squared volatility exhibit some variation, ranging from approximately 0.08 to 3.94, but taking most often values between 0.1 and 0.2; the correlation ρ between the driving Wiener processes is negative and very large in absolute value (except for one case), ranging from -0.85 to -0.98 ; the speed of mean reversion κ and the volatility η of the squared volatility, that also vary in a wide range, exhibit some degree of correlation between each other: small values of κ tend to be associated with small values of η . On each block we approximate the calibrated Heston density f by finite linear combinations of scaled and shifted Hermite functions, and compute their approximation errors in the norms L^2 , L^1 , and L^∞ , that are reported (in percentage terms of the corresponding norm of f) in Table 9. Errors are much higher than those obtained by the same methods for the test Heston

Table 10: Mean Absolute Relative Errors of Hermite Prices Calibrated on Heston Prices

For each block of put options of day 242 with the same time to maturity, the Hermite approximation $f_{3,p}^*$ is calibrated to the option prices implied by the Heston calibration, and the mean absolute relative error is reported. Each row refers to a block, where the first column contains the time to maturity in days, the second column the number of different strikes, and the third column the error in percentage points.

Maturity	Strikes	Error
4	29	16.8
10	24	4.87
13	20	4.95
13	9	0.146
17	12	0.302
32	36	2.11
60	19	1.09
88	22	1.78
88	11	1.65
186	7	4.79E-07
277	11	0.103
368	8	2.58

density considered above. A tentative explanation for this phenomenon, guided by inspecting closely a few cases, is that calibrated Heston densities tend to be peaked around zero, and for such functions Hermite approximations converge slowly in L^2 . Moreover, the approximations can display oscillations. This gloomy picture is completely changed if one calibrates Hermite estimators to the option prices implied by the calibrated Heston densities. Mean absolute errors of Hermite option prices estimates with respect to the implied Heston prices for each block are reported in Table 10. The accuracy of price estimation is very good, except for the first block, where, however, options have a very short time to maturity. Recall that, as already remarked, in this case the algorithm is induced to approximate the Heston density as closely as possible only on $]-\infty, \log K_{\max}]$, where K_{\max} stands for the highest strike price observed.

7.3 Out-of-sample performance on real data

We are now going to discuss the results of an extensive empirical study on the out-of-sample performance of the option price estimators discussed so far. The data set and the framework are the same used in [12], i.e. the data are raw option prices on the S&P500 for the whole year 2012, as mentioned above. For each trading day options are divided in blocks with the same time to maturity, and on each block instances of the parametric and nonparametric estimators of option prices discussed above are calibrated to all prices bar one, which is used as test price π . The prices estimated by the various calibrated parameters are then compared to the test price, and absolute relative errors are computed. That is, if $\hat{\pi}$ is an estimated price, the error $|\hat{\pi}/\pi - 1|$ is recorded. This operation is repeated until all prices in the block have been used as test prices. The same procedure is applied to every block of every day, obtaining samples of sizes between 40000 and 43500. Points of the empirical distribution of the absolute relative pricing errors are collected in Tables 11 and 12. In Table 11 we have also included, as terms of comparison, the simplest parametric model, that is the Black-Scholes model, and the simplest nonparametric model, that is the Black-Scholes model with interpolation on the implied volatility curve.

Table 11: Pricing errors of Black-Scholes, variance-gamma, and Heston estimators

The table reports selected quantiles of the empirical distribution of out-of-sample absolute pricing errors in percentage points of the Black-Scholes, variance-gamma, and Heston estimators. Figures in parentheses correspond to options with strike prices within the range of strike prices of options used to calibrate.

EMPIRICAL DISTRIBUTION OF PRICING ERRORS					
Black & Scholes					
Quantiles	$n = 1$	$n = 2$	$n = 3$	$n = 4$	$n = 5$
10%	10.5 (11.6)	10.4 (11.6)	10.4 (11.6)	10.4 (11.8)	10.5 (12.0)
25%	21.9 (22.6)	21.8 (22.5)	21.8 (22.6)	21.8 (22.7)	21.9 (22.8)
50%	38.0 (38.2)	37.6 (38.1)	37.4 (38.1)	37.3 (38.1)	37.2 (38.2)
75%	80.0 (80.0)	80.0 (80.0)	80.0 (80.0)	80.0 (80.0)	80.0 (80.0)
90%	93.5 (93.0)	93.3 (92.9)	93.3 (92.9)	93.3 (92.9)	93.3 (92.9)
95%	96.4 (96.0)	96.3 (96.0)	96.3 (96.0)	96.2 (95.9)	96.1 (95.9)
Black & Scholes with interpolated implied volatility					
Quantiles	$n = 1$	$n = 2$	$n = 3$	$n = 4$	$n = 5$
10%	0.1 (0.1)	0.1 (0.1)	0.1 (0.1)	0.1 (0.1)	0.1 (0.1)
25%	0.3 (0.2)	0.3 (0.2)	0.3 (0.2)	0.3 (0.3)	0.3 (0.3)
50%	1.4 (1.0)	1.3 (1.0)	1.3 (1.0)	1.3 (1.0)	1.3 (1.1)
75%	7.8 (4.5)	7.4 (4.5)	7.1 (4.5)	6.9 (4.6)	6.8 (4.7)
90%	30.3 (14.2)	28.7 (14.1)	27.3 (14.2)	26.4 (14.3)	25.6 (14.4)
95%	55.5 (25.7)	52.0 (25.6)	49.7 (25.7)	48.2 (25.8)	46.7 (25.9)
Variance-gamma					
Quantiles	$n = 1$	$n = 2$	$n = 3$	$n = 4$	$n = 5$
10%	0.7 (0.8)	0.7 (0.8)	0.7 (0.8)	0.7 (0.8)	0.8 (0.8)
25%	2.0 (2.0)	2.0 (2.0)	2.1 (2.0)	2.1 (2.1)	2.2 (2.1)
50%	6.1 (5.7)	6.0 (5.7)	6.1 (5.8)	6.1 (5.8)	6.2 (5.9)
75%	16.3 (15.1)	16.2 (15.1)	16.3 (15.2)	16.3 (15.3)	16.4 (15.4)
90%	35.5 (32.3)	35.2 (32.3)	35.1 (32.4)	35.0 (32.4)	35.0 (32.5)
95%	50.3 (46.7)	50.0 (46.6)	50.0 (46.7)	50.0 (46.6)	50.0 (46.7)
Heston					
Quantiles	$n = 1$	$n = 2$	$n = 3$	$n = 4$	$n = 5$
10%	0.4 (0.4)	0.4 (0.4)	0.4 (0.4)	0.4 (0.4)	0.4 (0.4)
25%	1.2 (1.2)	1.2 (1.2)	1.2 (1.2)	1.2 (1.2)	1.2 (1.2)
50%	4.0 (3.8)	4.0 (3.8)	4.0 (3.8)	4.0 (3.8)	4.1 (3.9)
75%	13.2 (12.4)	13.2 (12.4)	13.2 (12.4)	13.2 (12.5)	13.3 (12.6)
90%	34.1 (29.4)	33.8 (29.4)	33.6 (29.4)	33.4 (29.4)	33.1 (29.4)
95%	56.8 (45.7)	56.1 (45.7)	55.4 (45.6)	54.6 (45.6)	53.9 (45.5)
Test points	43469 (37760)	42755 (37522)	41815 (37052)	40830 (36461)	39834 (35797)

Table 12: Pricing errors of Hermite estimators

The table reports selected quantiles of the empirical distribution of out-of-sample absolute pricing errors in percentage points of the Hermite estimators $f_{n,p}^*$, f_n^* , and $f_{n,m}^*$.

EMPIRICAL DISTRIBUTION OF PRICING ERRORS					
$f_{n,p}^*$					
Quantiles	$n = 1$	$n = 2$	$n = 3$	$n = 4$	$n = 5$
10%	2.9 (3.2)	0.4 (0.4)	0.4 (0.5)	0.1 (0.1)	0.1 (0.2)
25%	8.8 (8.6)	1.5 (1.5)	1.6 (1.6)	0.5 (0.5)	0.5 (0.5)
50%	19.4 (18.3)	4.6 (4.4)	5.3 (5.0)	1.8 (1.7)	1.8 (1.7)
75%	37.2 (33.3)	12.2 (11.0)	13.3 (12.0)	6.6 (5.8)	6.5 (5.7)
90%	66.7 (60.8)	27.9 (23.5)	28.3 (23.5)	21.0 (16.3)	21.7 (16.5)
95%	80.0 (74.8)	47.5 (36.2)	46.5 (35.3)	44.9 (28.7)	50.3 (30.5)
f_n^*					
Quantiles	$n = 1$	$n = 2$	$n = 3$	$n = 4$	$n = 5$
10%	1.3 (1.4)	0.1 (0.2)	0.2 (0.2)	0.1 (0.1)	0.1 (0.1)
25%	4.2 (4.2)	0.5 (0.5)	0.6 (0.5)	0.4 (0.4)	0.4 (0.4)
50%	10.5 (10.1)	1.9 (1.8)	2.0 (1.9)	1.6 (1.5)	1.6 (1.5)
75%	22.7 (21.0)	6.8 (6.0)	6.8 (6.1)	6.4 (5.5)	6.5 (5.6)
90%	45.9 (40.5)	19.7 (15.9)	19.5 (15.8)	22.4 (16.4)	23.7 (17.3)
95%	63.1 (56.5)	37.4 (27.0)	38.0 (27.0)	51.3 (30.8)	59.8 (34.1)
$f_{n,m}^*$					
Quantiles	$n = 1$	$n = 2$	$n = 3$	$n = 4$	$n = 5$
10%	9.6 (10.8)	10.1 (11.3)	0.8 (0.9)	0.6 (0.7)	0.5 (0.6)
25%	20.6 (21.5)	23.5 (24.4)	2.5 (2.6)	2.2 (2.3)	1.8 (1.8)
50%	36.0 (36.8)	38.7 (39.3)	6.2 (6.3)	6.7 (6.7)	5.0 (4.7)
75%	79.0 (79.3)	75.0 (75.0)	15.1 (14.6)	15.7 (15.2)	11.8 (10.5)
90%	93.3 (92.9)	92.3 (91.7)	45.1 (37.0)	34.5 (31.4)	24.9 (20.4)
95%	96.3 (96.0)	95.7 (95.3)	66.7 (64.5)	56.4 (50.0)	39.5 (30.9)
Test points	43469 (37760)	42755 (37522)	41815 (37052)	40830 (36461)	39834 (35797)

Each panel of Table 11 contains five columns indexed by different values on n , where $n = k$, $k = 1, \dots, 5$ means that all blocks in the data set containing at most k options have been excluded from the computations. This explains the different sample sizes reported in the last row of the table. The rationale for this is that a model with k parameters calibrated to k or less prices obviously suffers of the well-known problem of overfitting. On the other hand, the empirical results show that the distributions of errors of all parametric models are quite robust with respect to the presence of small blocks, with minor variations showing up mostly at the 90% and 95% quantiles. The columns of Table 12 have the same interpretation, but in this case, if $n = k$, results are reported for estimators $f_{k,p}^*$, f_k^* , and $f_{k,m}^*$ in the first, second, and third panel, respectively.

Inspection of Table 11 reveals that both parametric estimators, i.e. the variance-gamma and the Heston model, are major improvements with respect to the elementary Black-Scholes model.² Unsurprisingly, the five-parameter Heston model displays lower average errors (up to the 90% quantile) than the three-parameter variance-gamma model. In particular, the median absolute relative error of the Heston model is 4%, while the corresponding error of the variance-gamma model is around 50% higher. For a detailed discussion of the results concerning the Hermite estimators (including others not considered here), we refer to [12].

In view of the discussion in §§7.1-7.2, we focus on the comparison between the variance-gamma model and the Hermite models with three parameters, that are $f_{1,p}^*$ and $f_{3,m}^*$, as well as between the Heston model and the Hermite models with five parameters, that are $f_{3,p}^*$, f_2^* , and $f_{5,m}^*$. The variance-gamma price estimator performs clearly better than the Hermite $f_{1,p}^*$ estimator, with the median error of the latter more than three times as large as the median error of the former, and the empirical error distribution of the latter dominating the one of the former. The picture is not as clear when the variance-gamma estimator is compared to the Hermite $f_{3,m}^*$ estimator: the quantiles of their respective empirical error distributions are very close up to and including the median, but the 75% quantile corresponding to the Hermite estimator is 15.1%, hence better than the same quantile corresponding to the variance-gamma, that is 16.3%. On the other hand, large estimation errors are less frequent for the variance-gamma than for the Hermite estimator. The comparison between the five-parameter estimators reveals some interesting and perhaps unexpected phenomena. Perhaps most importantly, it turns out that the empirical error of the Hermite estimator f_2^* is much lower, at all quantile levels, than the empirical error of the Heston model. This is indeed quite surprising, as the Heston model is tailor-made for financial returns, while the Hermite estimator is completely “agnostic”. Also the Hermite estimators $f_{3,p}^*$ and $f_{5,m}^*$ do not perform badly compared to the Heston estimator: both Hermite estimators have very close error up to the median, that are nonetheless higher than the errors of the Heston estimator. On the other hand, at higher quantiles, the Heston estimator performs worse than $f_{3,p}^*$, which in turns performs worse than $f_{5,m}^*$.

8 Concluding remarks

The empirical performance of both parametric and nonparametric estimators of option prices, focusing on variance-gamma and Heston models for the former and on expansions in Hermite functions for the latter, was evaluated by the off-sample relative pricing error using historical data on European options on the S&P500 index.

The main empirical observation is that a simple Hermite estimator with the same number of parameters as the Heston model outperforms the latter. This is remarkable as Hermite estimators are “uninformed” by their nature, while the Heston model is designed for financial assets. Moreover, as expected, the variance-gamma model, that depends on less parameters, has larger average pricing errors than the Heston model. These results highlight the trade-offs between

²On the other hand, the Black-Scholes model with interpolation on the implied volatility still has lower pricing errors than the two parametric methods. This is however not strictly relevant for the issues investigated here, as interpolating on a volatility curve is not a method depending on a fixed number of parameters.

the flexibility of nonparametric methods and the domain-specific precision of parametric models. Notably, the performance of Hermite estimators, combined with their simple and fast calibration, makes them a valuable tool for validation purposes.

A relevant question, that would be natural to address in future contributions, is whether suitable time-dependent extensions of Hermite estimators can still keep up with Heston estimators in the pricing of options with different times to maturity.

A Computational issues

We collect here, for completeness, some remarks about practical computational issues. All numerical computations have been done with `Octave` 9.1.0 on Linux, using `fminsearch` as minimization algorithm. The minimization problem to which calibration of a model amounts is often marred by the issue of local minima, and the cases of variance-gamma and Heston densities are not exception. In the variance-gamma case, calibration uses as starting point of the optimization the point $(\theta_0, \sigma_0, \alpha_0) = (0.1, 0.3, 2)$. Moreover, in order to avoid degenerate situations, a lower bound on σ equal to 0.05 was enforced. To price (European put) options in the Heston model, hence also for calibration purposes, we used the code provided by [5], that implements the steps described in §5. The starting point of calibrations is $(v_{00}, \theta_0, \rho_0, \kappa_0, \eta_0) = (0.02, 0.35, -0.5, 0.5, 0.3)$. On the other hand, Heston densities are approximated by an FFT implementation of Fourier inversion of the characteristic function, using code provided by [6].

References

- [1] D. Ackerer and D. Filipović. Option pricing with orthogonal polynomial expansions. *Math. Finance*, 30(1):47–84, 2020. doi:10.1111/mafi.12226.
- [2] H. Brézis and E. Lieb. A relation between pointwise convergence of functions and convergence of functionals. *Proc. Amer. Math. Soc.*, 88(3):486–490, 1983. doi:10.1090/S0002-9939-1983-0699419-3.
- [3] P. Carr and D. B. Madan. Option valuation using the fast Fourier transform. *Journal of Computational Finance*, 2(4):61–73, 1999. doi:10.21314/JCF.1999.043.
- [4] D. Duffie, D. Filipović, and W. Schachermayer. Affine processes and applications in finance. *Ann. Appl. Probab.*, 13(3):984–1053, 2003. doi:10.1214/aoap/1060202833.
- [5] J. C. Frei. Heston option pricing calibration. GitHub repository, 2016. URL: <https://github.com/jcfrei/Heston>.
- [6] G. Germano, 2024. Private communication.
- [7] S. L. Heston. A closed-form solution for options with stochastic volatility with applications to bond and currency options. *The Review of Financial Studies*, 6(2):327–343, 1993. URL: <http://www.jstor.org/stable/2962057>.
- [8] R. Lord and Ch. Kahl. Optimal Fourier inversion in semi-analytical option pricing. *Journal of Computational Finance*, 10(4):1–30, 2007. URL: <https://hdl.handle.net/10419/86580>, doi:10.21314/JCF.2007.171.
- [9] D. B. Madan, P. Carr, and E. C. Chang. The Variance Gamma Process and Option Pricing. *European Finance Review*, 2:79–105, 1998.
- [10] C. Marinelli. A note on variance-gamma processes, 2024. in preparation.

- [11] C. Marinelli. On certain representations of pricing functionals. *Ann. Finance*, 20(1):91–127, 2024. doi:10.1007/s10436-024-00438-5.
- [12] C. Marinelli and S. d’Addona. Nonparametric estimates of option prices via Hermite basis functions. *Ann. Finance*, 19(4):477–522, 2023. doi:10.1007/s10436-023-00431-4.
- [13] F. W. J. Olver et al. (eds.). NIST Digital Library of Mathematical Functions. <http://dlmf.nist.gov>, Release 1.1.6 of 2022-06-30. URL: <http://dlmf.nist.gov>.
- [14] M. Stephanou and M. Varughese. On the properties of Hermite series based distribution function estimators. *Metrika*, 84(4):535–559, 2021. doi:10.1007/s00184-020-00785-z.
- [15] Chenyu Zhao, M. van Beek, P. Spreij, and M. Ba. Polynomial approximation of discounted moments. *Finance Stoch.*, 2024. doi:10.1007/s00780-024-00550-4.